TURKISH NAVAL ACADEMY
NAVAL SCIENCE AND ENGINEERING INSTITUTE
DEPARTMENT OF COMPUTER ENGINEERING
MASTER OF SCIENCE PROGRAM
IN COMPUTER ENGINEERING

THREE PLANE APPROACH FOR 3D TRUE PROPORTIONAL NAVIGATION

Master Thesis

İNANÇ MORAN

Advisor: Assist. Prof. Deniz Turgay Altılar

İstanbul, 2005

© Copyright by Naval Science and Engineering Institute, 2005

CERTIFICATE OF COMMITTEE APPROVAL

THREE PLANE APPROACH FOR
3D TRUE PROPORTIONAL NAVIGATION

Submitted in partial fulfillment of the requirements for degree of

MASTER OF SCIENCE IN COMPUTER ENGINEERING

from the

TURKISH NAVAL ACADEMY

Author :

İnanç Moran

Defense Date : 13 / 07 / 2005
Approved by : 13 / 07 / 2005

Assist. Prof. Deniz Turgay Altılar (Advisor)

Prof. Ercan Öztemel (Defense Committee Member)

Assoc. Prof. Coşkun Sönmez (Defense Committee Member)

ABSTRACT (TURKISH)

ÜÇ BOYUTLU ORANTISAL SEYİR İÇİN ÜÇ DÜZLEM YAKLAŞIMI

Anahtar Kelimeler : Güdümlü Mermiler, Mermi Güdümü, Üç Boyutlu Gerçek Orantısal Seyir.

Bu tezde, yeni bir üç boyutlu güdüm yaklaşımı geliştirilmiş, bu yaklaşım geliştirilen bir benzeşim ortamında görsel olarak sınanmıştır. Söz konusu yöntem, Gerçek Orantısal Seyir (GOS) temeli üzerine kurulmakla beraber; GOS' e ait ivmelerin hesaplanması ve üç boyutlu ivme değerlerinin kartezyen koordinatlarda uygulanmasındaki farklılıklarla bu kuraldan ayrılmaktadır. Tasarlanan algoritma; *x*, *y*, *z* eksenleri ile tanımlı üç boyutlu uzayı, sırasıyla *xy*, *yz* ve *xz* ile adlandırılan birbirine dik üç düzleme ayırarak; kaçış–kovalama problemini analitik olarak bu düzlemlerde çözdükten ve gerekli ivme komutlarını ürettikten sonra, bu sonuçları üç boyutlu uzayda kullanmak üzere tekrar birleştirerek çalışmaktadır. Yörünge ve başarım çözümlemeleri VEGAS (Visual End-Game Simulation) adı verilen Görsel Son-Safha Simülasyonunda incelenmiştir. Başarım ölçütleri olan kaçırma mesafesi ve kesişme zamanı bakımından; önerilen yaklaşımın başarımının, 10-*g* manevra kapasitesine sahip hava hedefleri için yüksek olduğu sonucu elde edilmiştir. Bu tezde önerilen uyarlanabilir yaklaşım, aynı zamanda diğer Orantısal Seyir tipleri için de uygulanabilir.

ABSTRACT (ENGLISH)

THREE PLANE APPROACH FOR 3D TRUE PROPORTIONAL NAVIGATION

Keywords : Missile Guidance, Homing Missiles, 3D True Proportional Navigation

In this thesis; a new three-dimensional (3D) guidance approach is developed. The performance of this approach has been tested visually via developed simulation environment. Although this approach is based on True Proportional Navigation (TPN), it diverges when computing accelerations special to TPN, and putting 3D acceleration commands into practice in Cartesian coordinates. Proposed algorithm works by separating 3D space with axes x, y and z to three perpendicular plane *xy*, *xz* and *yz* respectively; after solving the pursuit-evasion problem analytically in these planes and computing required accelerations, rejoining the solutions to three-dimensional environment with respect to the geometric relationships. Trajectory and performance analysis are performed in our simulation software, VEGAS (Visual End-Game Simulation). It is verified that the performance of proposed approach is robust and effective in terms of the miss distance and interception time for the 10-g capacity aerial targets employing evasive maneuvers. The adaptive approach proposed in this thesis can be applied also to the other Proportional Navigation types.

DISCLAIMER STATEMENT

The views expressed in this thesis are those of the author and do not reflect the official policy or position of the Turkish Navy, Naval Academy, and Naval Science and Engineering Institute.

DEDICATION

I would like to thank my wife, Gamze, for all the support she has given to me through the whole duration of this study. Her constant encouragement and belief in my skills was invaluable.

I dedicate my thesis to Gamze.

ACKNOWLEDGMENTS

Assist. Prof. D. Turgay Altılar kindly supervised this thesis. I would like to extend my sincere appreciation to my advisor for his intelligent supervision, constructive guidance, genuine friendship and his encouragement in my study. I feel very fortunate to have had the opportunity to benefit from his brilliant insights and invaluable comments, which have been a great source of inspiration for me.

I thank my friend Remzi Akdağ for being a good team together and the cooperative study we started and completed successfully.

I would like to thank Prof. Süleyman Özkaynak for his support and the Naval Science and Engineering Institute for providing me with this research opportunity.

I would like to thank Mustafa Dinç for sharing his experiences and sources with me and providing the support for the growth and improving the quality of our work.

I would especially like to thank Ergin Altıntaş for his valuable ideas and comments on my study.

TABLE OF CONTENTS

LIST OF FIGURES

LIST OF FIGURES

LIST OF TABLES

LIST OF ABBREVIATIONS, ACRONYMS, AND SYMBOLS

APN	Augmented Proportional Navigation
ARM	Anti-Radiation Missiles
A_t	Area of missile nozzle throat
a_M	Total acceleration of the missile
a_{Mx}	Acceleration component of missile on x-axe
a_{My}	Acceleration component of missile on y-axe
a_{Mz}	Acceleration component of missile on z-axe
a_{pitch}	Vertical acceleration component of the missile
a_{yaw}	Lateral acceleration component of the missile
β	Flight path angle of the target (in 2D)
β_{xy}	Flight path angle of the target on xy plane
β_{xz}	Flight path angle of the target on xz plane
β_{yz}	Flight path angle of the target on yz plane
C_D	Drag coefficient
$C_{D\ body}$	Drag coefficient of body
$C_{D\ body\text{-}friction}$	Skin friction drag coefficient
$C_{D\ base\text{-}coast}$	Base drag coefficient in coasting flight
$C_{D\ base\text{-}powered}$	Base drag coefficient in powered flight
$C_{D\ body\text{-}wave}$	Drag coefficient due to shock waves
D	Drag force
d	Missile diameter
DOF	Degree-of-freedom
ECM	Electronic countermeasures
ε	Specific heat ratio
GTPN	Generalized True Proportional Navigation
g	Acceleration due to the gravity
I_{sp}	Specific impulse
J	Performance index in optimal guidance
HE	Heading error

id	Identification of the vehicles
χ_M	Heading angle of missile
γ_M	Flight path angle of missile
LOS	Line-of-sight
LOSR	Line-of-sight rate
L	Leading angle of missile
L_{xy}	Leading angle of missile on ***xy*** plane
L_{xz}	Leading angle of missile on ***xz*** plane
L_{yz}	Leading angle of missile on ***yz*** plane
l	Length of the missile
l_N	Length of missile nose
λ	Line-of-sight angle
λ_{xy}	Line-of-sight angle on ***xy*** plane
λ_{xz}	Line-of-sight angle on ***xz*** plane
λ_{yz}	Line-of-sight angle on ***yz*** plane
M	Mach number
m_M	Mass of the missile
$\dot{m}$	Mass flow rate
N'	Effective navigation ratio
NEE	No-escape envelope
n_c	Acceleration command of missile
n_{c_xy}	Acceleration command computed for ***xy*** plane
n_{c_xz}	Acceleration command computed for ***xz*** plane
n_{c_yz}	Acceleration command computed for ***yz*** plane
n_t	Acceleration command of the target
P_C	Chamber pressure
P_{Mx}	Position component of missile on ***x***-axe
P_{My}	Position component of missile on ***y***-axe
P_{Mz}	Position component of missile on ***z***-axe
PN	Proportional Navigation
PPN	Pure Proportional Navigation

$\boldsymbol{P_{Tx}}$	Position component of target on $\boldsymbol{x}$-axe
$\boldsymbol{P_{Ty}}$	Position component of target on $\boldsymbol{y}$-axe
$\boldsymbol{P_{Tz}}$	Position component of target on $\boldsymbol{z}$-axe
$\boldsymbol{P_{TMx}}$	Relative position component of the missile-target on $\boldsymbol{x}$-axe
$\boldsymbol{P_{TMy}}$	Relative position component of the missile-target on $\boldsymbol{y}$-axe
$\boldsymbol{P_{TMz}}$	Relative position component of the missile-target on $\boldsymbol{z}$-axe
$\boldsymbol{\rho}$	Air density
$\boldsymbol{\rho_\infty}$	Free stream density
$\boldsymbol{q}$	Dynamic air pressure
$\boldsymbol{R_C}$	Capture radius
$\boldsymbol{R_{TM}}$	Range between the target and the missile
$\boldsymbol{R_T}$	Range of target in PN Command Guidance
$\boldsymbol{R_M}$	Range of target in PN Command Guidance
$\boldsymbol{\acute{r}}$	Turning rate of the missile in Pursuit Guidance
$\boldsymbol{S_{xy}}$	$\boldsymbol{xy}$ plane of 3D space
$\boldsymbol{S_{xz}}$	$\boldsymbol{xz}$ plane of 3D space
$\boldsymbol{S_{yz}}$	$\boldsymbol{yz}$ plane of 3D space
$\boldsymbol{S_M}$	Reference area of the missile
$\boldsymbol{ss}$	Speed of sound
STT	Skid-to-Turn
TPA	Three Plane Approach
$\boldsymbol{T_M}$	Thrust force of missile
TPN	True Proportional Navigation
$\boldsymbol{t_f}$	Flight time
$\boldsymbol{\theta_M}$	Line-of-sight angle of missile in PN Command Guidance
$\boldsymbol{\theta_T}$	Line-of-sight angle of target in PN Command Guidance
VEGAS	Visual End-Game Simulation
$\boldsymbol{V_c}$	Closing velocity
$\boldsymbol{V_{Cxy}}$	Closing velocity in $\boldsymbol{xy}$ plane
$\boldsymbol{V_{Cxz}}$	Closing velocity in $\boldsymbol{xz}$ plane
$\boldsymbol{V_{Cyz}}$	Closing velocity in $\boldsymbol{yz}$ plane

V_e	Nozzle exit velocity
V_M	Velocity magnitude of missile
V_{Mx}	Component of missile velocity vector on x-axe
V_{My}	Component of missile velocity vector on y-axe
V_{Mz}	Component of missile velocity vector on z-axe
V_{Mxy}	Projection of missile velocity vector onto xy plane
V_{Mxz}	Projection of missile velocity vector onto xz plane
V_{Myz}	Projection of missile velocity vector onto yz plane
V_T	Velocity of the target
V_{Tx}	Component of target velocity vector on x-axe
V_{Ty}	Component of target velocity vector on y-axe
V_{Tz}	Component of target velocity vector on z-axe
V_{Txy}	Projection of target velocity vector on to xy plane
V_{Txz}	Projection of target velocity vector onto xz plane
V_{Tyz}	Projection of target velocity vector onto yz plane
V_∞	Free stream velocity
W	Weight

I. INTRODUCTION

A. MOTIVATION

At the beginning of this study, general guided missile and guidance law concepts are revised. Previously, surface-to-surface missiles (SSM), and then air-to-air (AAM) missiles' guidance issues are considered. While looking into air-to-air missiles, it is realized that the most crucial phase of an air encounter is terminal phase, the last seconds of it; because the success or failure of entire mission is determined in this phase. With this motivation, we started to study Proportional Navigation (PN) that is used as the terminal phase guidance law in AAM.

After getting the basics of PN, a new 3D guidance law approach based on True Proportional Navigation (TPN) is developed. To evaluate the performance of this approach visually, a simulation environment is constructed, named VEGAS.

In simulations, one degree-of-freedom modeling is taken into consideration and aerodynamic forces and constraints such as, thrust, drag, weight and maximum acceleration limits are included into missile equations of motion.

The target is assumed as high-g capacity fighter aircraft (F-16). Modeling of the target aircraft and structure of "evader" module in VEGAS are implemented by Akdağ [1]. Developed guidance law is tested on the targets which are employing basic evasive maneuvers such as Immelmann, Horizontal-S, Split-S, Barrel Roll and Linear Acceleration. It is verified that the developed approach is effective in terms of performance metrics such as interception time and miss distance.

B. TACTICAL MISSILE GUIDANCE

The missiles may be discussed under two general titles concerned with their concept:

- strategic ballistic missiles
- tactical guided missiles

Strategic ballistic missiles are separated from tactical guided missiles by their traveling much longer distances and being designed to intercept stationary targets whose location is known exactly.

The need for tactical missile guidance systems were born at the end of World War II as a result of effective kamikaze attacks. After the war, it was obvious that naval guns using unguided shells were not adequate for shooting down aircrafts making suicidal attacks against ships. Today, modern missile systems use guidance concepts work well not only against stationary targets but also are effective against harder targets like aircrafts employing evasive maneuvers.

A tactical active homing missile acquires the target with its seeker and guides all the way to intercept [2]. Guidance is the action of determining the course, attitude and speed of the missile to pursuit the target. Primary functions of the elements that constitute a guidance system are data acquisition, data processing and correction.

A guidance system acquires data from various on-board or external sensors and generates relevant signals or set points for its control system. Guidance issues are mainly determined by the characteristics and the location of both target and the missile, and the environmental conditions. Since 1944, various control and guidance techniques have been developed to improve the missile performance. The fundamentals of guidance were extensively covered by Locke [3] and navigation, guidance and control of airborne systems have been reported in the literature [4, 5, 6].

Many of the current operational guided missiles employ PN as the guidance law for the terminal phase. PN has been proved to be a useful guidance scheme in many air-to-air and surface-to-air homing systems for the interception of airborne targets [2, 7, 8, 9].

The major advantage of PN is its simplicity of implementation in missile systems. PN requires low level of target information thus simplifying missile sensor requirements and improving effectiveness. Theoretically, True Proportional Navigation (TPN) guidance law generates acceleration commands perpendicular to the instantaneous missile-target line-of-sight (LOS), and proportional to the line-of-sight rate (LOSR) and closing velocity, $\boldsymbol{V_c}$.

The fundamentals of PN law and detailed exposition about its schemes are analyzed in Section II. A novel approach to the solution of guidance in 3D environment is raised in this study. The aerodynamic forces and the effects of those on missile are also considered while employing the proposed approach.

C. CONTRIBUTION OF THE THESIS

In this thesis, a comprehensive research is done on missile guidance; PN based guidance laws and the related issues of missile aerodynamics. As the main contribution of this thesis; a novel guidance approach for 3D missile guidance is developed, which is effective against high-g capability fighter aircrafts that employ evasive maneuvers.

Furthermore, VEGAS, visual simulation software, is constructed as a production of this thesis and Akdağ's [1]. From the viewpoint of a missile, pursuer module of VEGAS includes very large number of missile parameters. Thus, it is possible to evaluate the effectiveness of different missile configurations by changing only the parameters of the "pursuer" module of VEGAS.

D. STRUCTURE OF THE THESIS

The rest of the thesis is organized as follows:

Chapter II contains brief information about history and development of guided missiles, homing types, guidance and mostly used guidance laws, especially PN and its variants. Analytical solutions of True Proportional Navigation and Proportional Navigation Command Guidance are given in detail.

In Chapter III, aerodynamic issues about the missile guidance are discussed. To begin with atmospheric properties; equations of aerodynamic forces act on a missile such as thrust, drag and weight are explained in detail with related physical missile parameters. The derivation of missile drag coefficients at different Mach numbers, the missile propulsion alternatives and the derivation of thrust force are also explained.

In Chapter IV, a novel three-dimensional guidance law approach, named Three Plane Approach (TPA) is developed as the main contribution of the thesis.

In Chapter V, the simulation tool developed particularly to visualize and test proposed algorithm which is named as the Visual End-Game Simulation, VEGAS is introduced. The expositions about the design and module features, the construction and flow of the simulation are described.

Performance evaluation of the Three Plane Approach is given in Chapter VI. Missile and target models, equations of motion modeling and simulation scenarios are discussed. Numerical simulation results related to missile performance metrics are included.

In Chapter VII, simulation results of proposed approach are discussed and comparisons with other methods are given to conclude the thesis. Future research topics are also mentioned.

II. BACKGROUND INFORMATION AND RELATED WORK

In this chapter, guided missile history and development, homing types, guidance and guidance laws, especially PN and its variants are presented as a background of our work. Analytical solution of True Proportional Navigation, given at the end of this chapter, builds a base on our guidance approach, TPA.

Although they were never used during World War I, the British “*A.T.*” and the U.S. “*Kettering Bug*“ missiles are considered to be the first guided missiles in the history. British guided missile studies began in 1914. The name of the project was A.T., "*Aerial Target*". “*A.T.*” concept missiles were intended to determine the feasibility of using radio signals to guide a flying bomb to its target. Two *A.T.* test flights were conducted in 1917. Although both missiles crashed due to engine failure, it was determined that radio guidance was feasible [9].

Under the direction of Charles Kettering, development of the “*Kettering Bug*“ missile began in 1917. The “*Kettering Bug*” was made of wood and weighting just 600 pounds, including a 300 pounds bomb as payload. It was successfully demonstrated in 1918. However, World War I ended before the guided missile could be placed into production.

In 1937, German rocket developing center was located to a top-secret base at “*Peenemunde*” on the Baltic Coast. The first task of engineers was to develop and test a new rocket called the “*A-3*”. Although the propulsion system of the “*A-3*” functioned well, its inertial guidance system did not.

Although Germany produced and deployed a number of rocket and missile weapons during World War II, the potency of their weapons was based on the "*V*" weapons. The “*V-1*” was the first of the numbered *V*-weapons. “*V-1*” was launched from a ramp, and was unguided. After “*V-1*” was launched, it flew a preset course until a switch cut off its engine, causing the *V-1* to simply fall on where it was.

Since the “*V-1*” was unguided, the weapon rarely hit a specific target. It had a top speed of about 390 miles per hour, so could be intercepted by fighter aircraft or destroyed by anti-aircraft artillery.

Wartime production of the “*V-2*” began at the “*Peenemunde Experimental Center*”. The guidance section contained an automatic pilot, accelerometer and radio equipment. The automatic pilot was made up of two electric gyroscopes that stabilized the rocket's pitch, roll and yaw motions.

The “*Rheintochter*” (*R-1*) was a surface-to-air missile also developed in Germany during World War II. [2,9]. This two-stage radio controlled missile weighted 4000 pounds. This missile was inefficient since the target aircrafts flew above the range of it at the time. “*Rheintochter 3*” was an improved version of “*R-1*”.

“*Schmetterling*”, referred to as the “*V-3*”, was launched from rotatable platforms and employed two externally mounted solid-fueled booster engines and a liquid-fueled sustainer engine.

“*Wasserfall*” was a missile based on the “*V-2*”. It was essentially a 1/3 scale version of the *V-2*. The missile was radio-guided and was controlled by a set of four control fins. It could carry a 674 pounds explosive payload detonated by radio command from the ground.

“*Hs.298*” named, air-to-air, radio controlled guided missiles were developed in Germany during World War II. This air-to-air concept, solid-fueled missile was also employing a radio guidance system. In 1944, three missiles were test-flown from *JU-88G* aircraft and they all failed to hit the targets. Therefore, these missiles couldn’t be used in any air combat [2, 9].

Since Japanese kamikaze attacks posed a significant threat to U.S. Navy vessels, two important research programs about surface-to-air concept started at the end of the World War II. *Little Joe* missile was controlled by a gyroscopic stabilizer combined with commands from a radio guidance/optical tracking system. Its explosive warhead was designed to detonate by a proximity fuse as it approached its target.

Development of “*Lark*” missile began in 1944 on a schedule which was accelerated to accommodate for weaknesses in the *Little Joe* program. The “*Lark*” was launched by two solid-fueled booster engines and powered in flight by a tandem of two liquid-fueled sustainer engines, one of which was intended to be used as a back-up if the missile failed to reach its desired speed. It had four fins and four wings, employed a radio-guided mid-course correction system and a semi-active homing device [9].

After giving the early history of the guided missiles, main topics of the modern guidance systems such as homing types, guidance laws and specifically Proportional Navigation are given in the rest of this section.

Contemporary technologies enabled essential increase in range, maneuverability and velocity, variety of launch platforms, homing types and extended guidance laws. Up to date systems are designed for the specific type of the target to perform more accurately. To give an example, a missile system that is used in surface-to-surface engagement can not be expected to be matching with the one that used against aerial targets. Modern guidance topics are given below.

A. HOMING TYPES OF GUIDED MISSILES

1. Command Guidance

In command guidance, a missile seeker is not required. A radar that is external to the missile both transmits and receives the radar signals. After the guidance problem is solved and the required acceleration command is generated, command is up-linked to the missile to tripper required actions via the flight control system. While intercept takes place further away from the radar, measurement accuracy and hence the guidance accuracy is reduced with increasing range [10]. This can be considered as disadvantage of command guidance.

2. Beam Riding

Beam riding is another form of command guidance. The object of the beam riding is to fly the missile along a radar or laser beam that is continuously pointed at the target. Since the missile is attempting to fly along a moving beam, the missile guidance commands must be a function of the angular deviation of the missile from the beam. If the beam is always on the target and the missile is always on the beam, the missile will intercept the target. Beam Riding principle is one of the first methods used because of its simplicity and ease of implementation. Pursuit guidance, explained in Section II.B.3.b, is usually used in Beam Rider systems as guidance law. Talos, Terrier and Sea Killer missiles could be named as examples of this kind of homing system [10].

3. Semi-Active Homing

In Semi-Active homing system, a radar external to the missile, usually in the launch platform, transmits signal on the target just like an illuminator, and the missile receives the reflections of this signal and solves the guidance problem by itself. As a disadvantage; semi-active homing systems are vulnerable to Anti-Radiation Missiles (ARM) which usually fired from fighter aircrafts. Most of the semi-active missiles use PN for guidance [10]. Some of the contemporary guided missiles such as “SA-6” (Gainful), “SA-11” (Gadfly), “MIM-23” (Hawk), “AIM-7” (Sparrow), “AA-7” (Apex), “SM-1” are those using semi-active homing.

4. Tracking via Missile

In this type of homing, the combination of command guidance and semi-active homing is used. On the launch platform, there is a tracking radar, transmitting signals and receiving signal reflections from the target. While getting the target information from this channel, missile sends information of the target by using downlink. After processing the seeker signal data and correlating with other relevant data, a command is up-linked to the missile.

Electronic counter-counter measures are enhanced in tracking via missile. ”MIM-104“ (Patriot) and “SA-10” (Grumble) missiles are the examples of tracking via missile type.

5. Passive Homing

The missile is homing on the radiation emitted from the target. The missile seeker only receives radiation from the target without transmitting any signal. To give example; “SA-7, 13, 16” (Stinger), “AA-2, 9” (Sidewinder) and “Penguin” missiles are the IR guided passive homing missiles, “ALARM”, “HARM” and “AS-12” (Kegler) missiles are ARM type (Anti-Radiation Missile) passive homing missiles [10].

6. Active Homing

In active homing, missile seeker includes a transmitter and provides the data required for the guidance by receiving signals reflected from the target. The virtue of active homing is that measurement accuracy in the course of interception is continually improving because the missile, with onboard seeker, is getting closer to the target as the missile goes on. Most of the active homing missiles use Proportional Navigation as guidance law. “SSN-25” (Switchblade), “MM-38” (Exocet), “AIM-120” (AMRAAM), “AIM-54” (Phoenix), “AA-12” (Adder) and “RGM-84” (Harpoon) are the example missiles which use active homing.

B. GUIDANCE

The basic definition of guidance is the action of determining the course, attitude and speed of the missile, to pursuit the target. Guidance is different than navigation in the sense that absolute information concerning the present or future location of the target is not required for interception for the guidance.

In other words, if the current location and the destination known precisely, navigation is the method for getting to the destination; however, if either the current location or the destination is not known precisely, guidance is the method of getting you there.

From the viewpoint of a control approach, guidance is a special type of computational algorithm that is placed in a flight control system, also called autopilot, to accomplish an intercept [6].

Holding the target in no-escape envelope (NEE) is one of the main goals of guidance. No-escape envelope is the region from which the target fails to escape from the missile. Typically, modern missiles employ radar or an infrared sensor to provide measurements of the target location. The guidance law of the homing system translates the measurements into guidance commands, which the guidance system then translates into commands for the control surface actuators [11]. Block diagram of a typical missile guidance system is shown in Fig. 1.

In an air encounter, target makes evasive maneuvers against missile. Relative positions of missile and target mainly constitute the engagement geometry. To be able to track the target, the target has to be in the field of view of the missile's seeker head. The physical limit for the seeker cone angle, the angle between the tracking boresight axis and the missile centerline, is typically about ±40 to ±60 degrees. Missile seeker tracks the target and measures the target data such as line-of-sight angle, closing velocity. But an error signal within the seeker electronics provides a noisy set of data. Noise filter smoothes the noisy seeker signal data in order to provide a clear estimate of target data. In guidance section, a guidance command is generated, based on actual guidance law, by using the data taken from the noise filter output. The flight control system or autopilot gets the missile to maneuver with respect to these guidance commands.

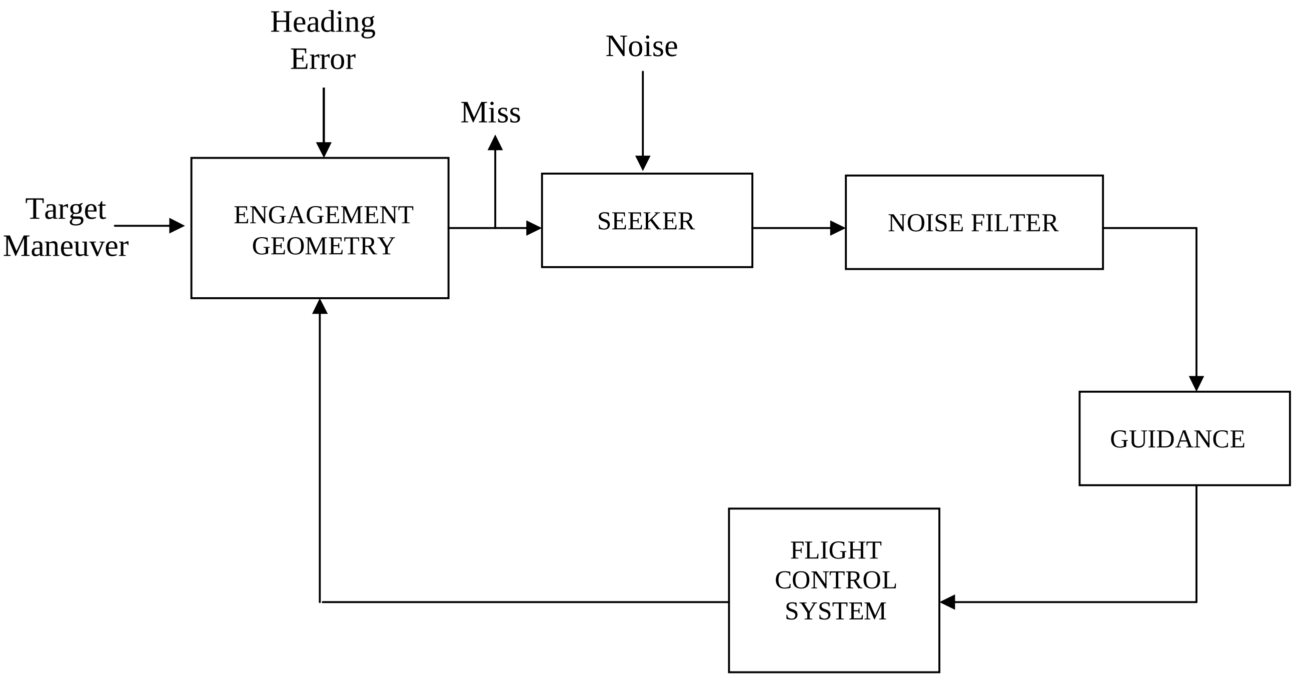

Figure 1 Block Diagram of Missile Guidance System

1. Guidance Phases

For endo-atmospheric tactical missiles, which fly in the boundary of atmosphere, there are generally three phases of guidance. These are:

- boost phase
- midcourse phase
- terminal phase

The first part of the trajectory is called the *boost phase*, which occurs for a very short time with an enormous thrust force to give initial velocity to the missile. At the completion of this phase, *midcourse phase* is initiated. The function of the *midcourse phase* is to place the missile at such a point that the target is within the acquisition range of its seeker and the missile seeker pointed in an appropriate direction with respect to the target.

Last seconds of the engagement constitute the *terminal phase*, which is most crucial phase since its success or failure determines the success or the failure of the entire mission [12].

In the *terminal phase*, the missile locks on to the target; acquires reliable tracking data, such as the missile-target relative range, closing velocity, line-of-sight (LOS) angle, LOS angle rate (LOSR) and efforts to close the distance to the target as quickly as possible under the constraints of its fuel and maneuver limitations.

2. Miss Distance

The point of closest range between the missile and the target is defined as *Miss Distance* [2]. In all of the guidance types, the main goal is to make the miss distance zero, or acceptable non-zero values within capture radius. The *Miss Distance* is directly related with; specific target maneuvers, active and passive ECM, missile and target engagement geometry dynamics. *Miss Distance* is determined by integrating incremental flight path errors over entire missile flight (Fig.2).

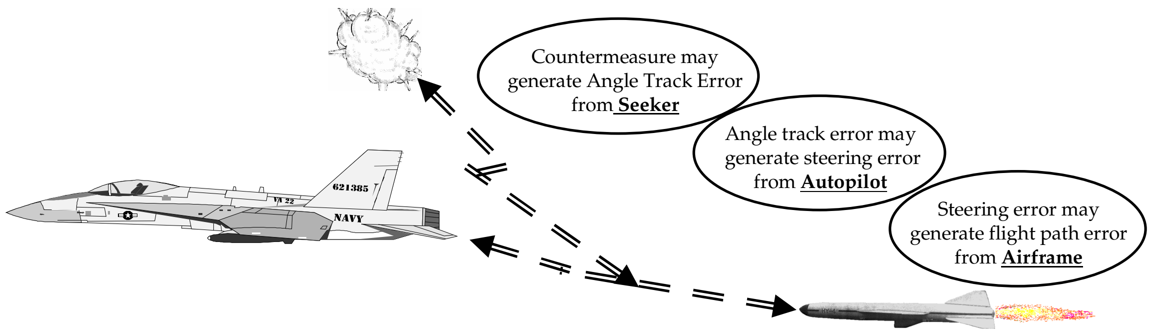

Figure 2 Miss Distance Determination

3. Guidance Laws

Many different guidance laws have been employed exploiting various design concepts over the years. Currently, the popular terminal guidance laws involve line-of-sight (LOS) guidance, line-of-sight rate (LOSR) guidance, Pursuit Guidance, Optimal Guidance Law [13, 14, 15, 16, 17] and Proportional Navigation (PN) [2, 3, 18].

Guelman [19] obtained the closed-form solution for True Proportional Navigation (TPN) against a non-maneuvering target. Shukla et al. derived the general linearized solution of PN [20]. Various solutions for Pure Proportional Navigation were given by Mahapatra et al. [21] and Becker [22]. Yuan et al. [23, 24] also presented closed-form solutions for TPN against both maneuvering and non-maneuvering targets.

Recently, many advance strategies have been implemented to generate different guidance laws. Rajasekhar et al [25] uses fuzzy logic to implement PN law. The fuzzy law generates acceleration commands for the missile using closing velocity and LOS rate as input variables. The input data is fuzzified and their degree of membership to the output fuzzy set is evaluated which is then defuzzified to get the acceleration command.

A fuzzy based guidance law for missiles has also been proposed by Creaser et al, [26], using an evolutionary computing based approach. The proposed law uses a genetic algorithm to generate a set of rules for the missile guidance law.

Menon et al. [27] uses fuzzy logic weightings to blend three well-known guidance laws to obtain enhanced homing performance. The composite law evaluates the weights on each of the guidance laws to obtain a blended guidance command for the missile.

In [28], the authors have implemented an H∞ based guidance law. Unlike other guidance laws, it does not require the information of target acceleration, while ensuring acceptable interceptive performance for arbitrary target with finite acceleration.

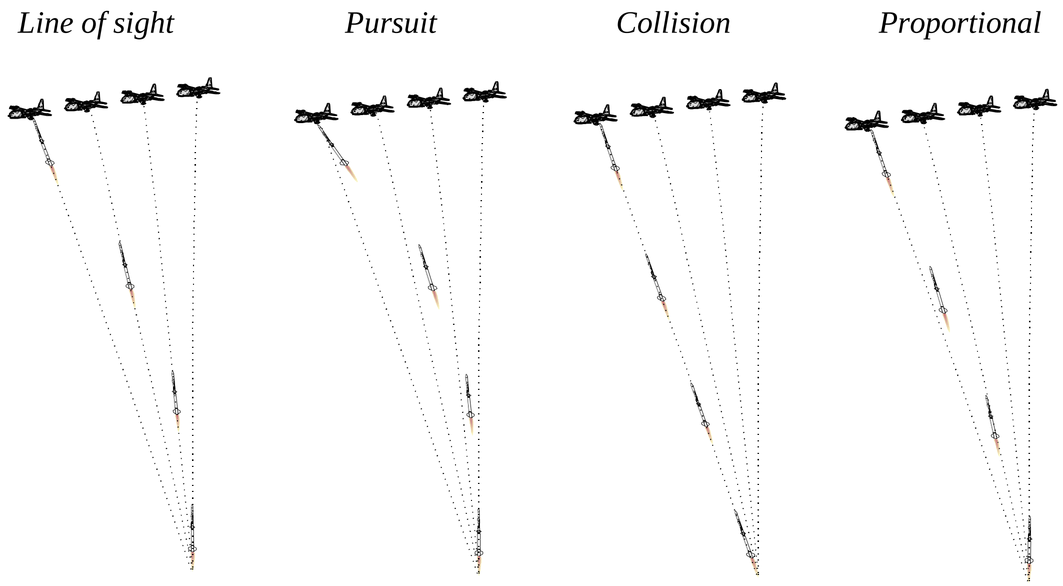

Figure 3 Guidance Types

a. Line-of-Sight (LOS) Guidance

LOS guidance is the base of widely used guidance strategy today. Actually, almost all guidance laws in use today have some form of LOS guidance because of its simplicity and ease of implementation. The LOS guidance employs the line-of-sight angle, $\boldsymbol{\lambda}$, angle between the missile and the target which can easily be evaluated using Eq.1.

$$\lambda = \arctan \frac{(Y_T - Y_M)}{(X_T - X_M)} \tag{1}$$

where (X_M, Y_M), (X_T, Y_T) are the missile and target position coordinates in two dimensions respectively.

The objective of the guidance system is to keep the missile to lie as nearly as possible on the LOS (Fig.3). Since a missile ideally always lies on the line joining it to the target, the flight path will be a curved one. LOS guidance does not work well with maneuvering targets. Also, the interception time is high which can be abridged using different strategies as discussed in the following.

b. Pursuit Guidance

Pursuit Guidance is a guidance law that is not as effective as Proportional Navigation. However it does not require some of the hardware essential for PN such as Doppler radar. In this guidance law, an attempt is made to keep the turning rate of the missile equal to the line-of-sight rate. The turning rate of the missile, $\acute{r}$ is related to the missile acceleration n_c and velocity V_M as in Eq.2.

$$\acute{r} = \frac{n_c}{V_M} \tag{2}$$

The pursuit guidance law could be expressed as:

$$n_c = V_M \,.\, \acute{r} \tag{3}$$

When expressed in the terms of LOS rate, pursuit guidance seems to be very similar to Proportional Navigation except that the acceleration depends on missile velocity rather then the closing velocity and the gain is unity rather than an effective navigation ratio. It is effective for non-maneuvering targets. Pursuit guidance trajectory is longer than the one for PN since the algorithm yields to a tail-chase (Fig.3). Moreover pursuit guidance requires higher acceleration values than PN does.

Acceleration profile for pursuit guidance is monotonously increasing whereas for PN it is monotonously decreasing.

c. Optimal Guidance

Recently, great interest has been shown in using optimal control theory in the missile guidance problem. Missile-target engagement time and the energy needed to complete the interception course of engagement are to be minimized by utilizing optimal control. Tsao and Lin [17] proposed an optimal guidance law for short-range homing missiles to intercept highly maneuverable targets. The guidance problem that needs to be solved for the interception is to find the optimal missile trajectory such that the total time for the interception is minimized. A performance index, ***J***, used in the proposed optimal law is:

$$\boldsymbol{J} = \boldsymbol{t_f} = \int_0^{\boldsymbol{t_f}} \boldsymbol{dt} \qquad (4)$$

where $\boldsymbol{t_f}$ is the interception time. The proposed guidance law achieves the best performance in terms of miss distance and interception time in comparison to the True Proportional Navigation (TPN) guidance.

However, a major disadvantage of this law is that the target's future trajectory must be known in advance which is impossible to evaluate in a realistic engagement environment. Although future trajectory can be estimated more accurately with the development of sensors and estimators, the complexity and the cost of the guidance system increase as well as uncertainties or errors.

d. Proportional Navigation (PN) Guidance Law and Its Variants

Proportional Navigation (PN) has been known since World War II. and applied by the Germans at *Peenemünde*. The “*Lark*” missile, which was successfully tested in 1950, was the first missile to use PN.

Proportional Navigation was studied by C. Yuan et al. at RCA Laboratories during under the support of the U.S. Navy [29]. Proportional Navigation was extensively studied at *Hughes Aircraft Company* and implemented for a tactical missile using a pulsed radar system. PN was examined at *Raytheon* and implemented in a tactical continuous wave radar homing missile [30]. After World War II., the U.S. work on PN was declassified and first appeared in [31].

Today, guidance commands proportional to the LOS angle rate are generally used by most of the high-speed missiles to correct the missile course in the guidance loop [11, 32]. In PN, the acceleration of the missile is, perpendicular to the velocity of the missile (PPN) or perpendicular to the line-of-sight (TPN), and proportional to the observed line-of-sight rate (LOSR) and the closing velocity, $\boldsymbol{V_c}$. The line-of-sight rate (LOSR) is the angular velocity of the line connecting the missile and the target. Hence, the change in the heading of the missile is also proportional to the LOSR.

In other words, velocity vector of the missile is rotated at a rate that is proportional to the rotation rate of the line joining the missile and the target (LOSR). In essence, PN is simply a proportional controller that regulates the LOSR to zero. The idea is that if LOSR is zero; the target and the missile are on collision course.

Actually in an encounter, the missile seeker attempts to track the target and measures the line-of-sight angle (LOS) and the closing velocity, $\boldsymbol{V_c}$. A guidance command is generated, based on the proportional navigation guidance law.

The flight control system enables the missile to maneuver in such a way that the achieved acceleration matches the acceleration commands from the guidance law. Endo-atmospheric missiles move control surfaces to get acceleration while exo-atmospheric interceptors use divert engines to get the appropriate acceleration.

Proportional Navigation is the most common and effective technique that seeks to nullify the angular velocity of the LOS angle. The missile heading rate is made proportional to the LOS rate. The rotation of the LOS is measured by a sensor either onboard or located at a ground station, which causes commands to be generated to adjust the direction of the missile in the direction of the target. Mathematically PN law can be stated as:

$$\boldsymbol{n_c = N' \cdot V_c \cdot \dot{\lambda}} \tag{5}$$

where, $\boldsymbol{n_c}$ is the acceleration command, $\boldsymbol{N'}$ is the effective navigation ratio, $\boldsymbol{V_c}$ is the closing velocity, $\boldsymbol{\dot{\lambda}}$ is the LOS angle rate. The advantage of using PN guidance over LOS guidance is that the interception time can be greatly reduced by adjusting the effective navigation ratio.

There are variations of PN such as True PN [19], PN Command Guidance [2], Augmented PN [2], Generalized TPN [33], Pure PN [22]. These variations and their differences are given below.

(1) True Proportional Navigation

As briefly stated before, True Proportional Navigation (TPN) guidance law generates acceleration commands, perpendicular to the instantaneous missile-target line of sight (LOS), which are proportional to the line-of-sight rate (LOSR) and the closing velocity as shown in Eq.5.

$$\boldsymbol{n_c = N' \cdot V_c \cdot \dot{\lambda}}$$

where $\boldsymbol{n_c}$. is the acceleration command, $\boldsymbol{N'}$ is effective navigation ratio, a unitless constant for gain to be set by designer; $\boldsymbol{V_c}$ is the missile-target closing velocity and $\dot{\lambda}$ is the time derivative of the LOS angle.

In tactical active homing missiles that using PN as guidance law; seeker provides measurement of the line-of-sight rate, $\dot{\lambda}$ and radar provides closing velocity, $\boldsymbol{V_c}$. Computed Proportional Navigation acceleration commands are implemented by tactical missile's control surfaces to obtain the required lift for the missile. A two-dimensional missile-target engagement geometry for Proportional Navigation is shown in Fig. 4.

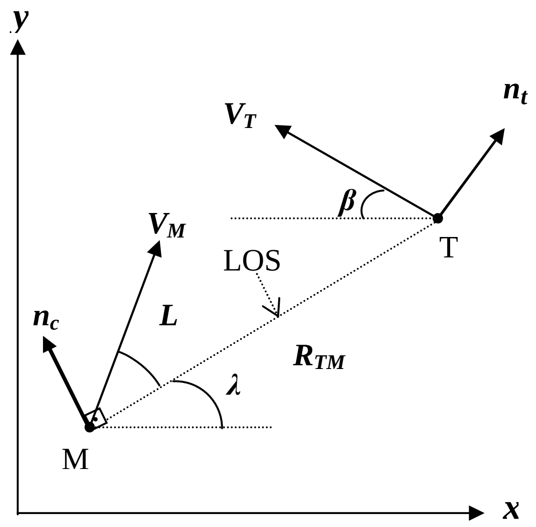

Figure 4 Two dimensional Missile-Target Engagement Geometry for TPN

In Figure 4, the capital M and T denotes the missile and the target respectively. The imaginary line connecting the missile to the target is the line-of-sight (LOS). LOS makes an angle of $\boldsymbol{\lambda}$ with respect to the x-axe. The length of the LOS called range and denoted $\boldsymbol{R_{TM}}$. Missile velocity vector, $\boldsymbol{V_M}$ makes an angle of $\boldsymbol{L}$ with respect to LOS angle. The angle $\boldsymbol{L}$ is called the missile lead angle. $\boldsymbol{V_T}$ is the target velocity vector. $\boldsymbol{\beta}$ is the flight path angle of the target and $\boldsymbol{n_c}$ is the acceleration magnitude which is generated by PN guidance law.

Considering the geometry drawn in Fig.4; details of the missile-target engagement model in two-dimensional (2D) space are presented below.

The effective navigation ratio, $\boldsymbol{N'}$, is related to the relative velocity between the missile and the target and derived from Eq.6 [10]:

$$3.\ \frac{\boldsymbol{V_M - V_T}}{\boldsymbol{V_M}} < \boldsymbol{N'} < 3.\ \frac{\boldsymbol{V_M + V_T}}{\boldsymbol{V_M}} \tag{6}$$

The missile will stay on the collision triangle if target does not change its heading or speed in this time interval, once $\boldsymbol{L}$ is computed. The point of closest range of the missile and the target is miss distance. It is desired to make the miss distance zero or acceptable non-zero values that will keep the target in explosion impact range.

The initial angle of the missile velocity vector with respect to the line-of-sight (LOS) i.e. the missile lead angle $\boldsymbol{L}$ can be computed by applying of the law of sine:

$$\boldsymbol{L = \arcsin \frac{V_T.\ \sin(\beta+\lambda)}{V_M}} \tag{7}$$

The components of the target velocity vector, $\boldsymbol{V_T}$ on $\boldsymbol{x}$ and $\boldsymbol{y}$ axis are given in Eq.8 and Eq.9 respectively. Negative sign in the term $\boldsymbol{V_{Tx}}$ comes from the projection of $\boldsymbol{V_T}$ on to the $\boldsymbol{x}$-axe as seen in Fig.4.

$$\boldsymbol{V_{Tx} = -\ V_T\,.\ \cos\beta} \tag{8}$$

$$\boldsymbol{V_{Ty} = \quad V_T\,.\ \sin\ \beta} \tag{9}$$

As the first derivative of the displacement (position) vector gives the velocity vector and consecutively the first derivative of the velocity vector gives the acceleration vector, the following differential equations having the components of the target and missile position can be derived.

Note that subscripts T and M indicate target and missile where $\boldsymbol{x}$ and $\boldsymbol{y}$ indicate the related axis. Considering target position components, differential equations are:

$$\dot{\boldsymbol{P}}_{Tx} = \boldsymbol{V}_{Tx} \tag{10}$$

$$\dot{\boldsymbol{P}}_{Ty} = \boldsymbol{V}_{Ty} \tag{11}$$

Similarly, considering the missile position components:

$$\dot{\boldsymbol{P}}_{Mx} = \boldsymbol{V}_{Mx} \tag{12}$$

$$\dot{\boldsymbol{P}}_{My} = \boldsymbol{V}_{My} \tag{13}$$

And the missile velocity components:

$$\dot{\boldsymbol{V}}_{Mx} = \boldsymbol{a}_{Mx} \tag{14}$$

$$\dot{\boldsymbol{V}}_{My} = \boldsymbol{a}_{My} \tag{15}$$

where $\boldsymbol{a}_{Mx}$ and $\boldsymbol{a}_{My}$ are the components of missile acceleration, $\boldsymbol{n}_c$, which will be obtained by the PN law.

Considering that any vector constitutes two projections on two perpendicular axes. ($\boldsymbol{x}$ and $\boldsymbol{y}$ for this case), $\boldsymbol{R}_{TM}$ can be defined as follows:

$$\boldsymbol{R}_{TM} = \sqrt{\boldsymbol{P}^2_{TMx} + \boldsymbol{P}^2_{TMy}} \tag{16}$$

where, relative position components are P_{TMx} and P_{TMy} are:

$$\boldsymbol{P}_{TMx} = \boldsymbol{P}_{Tx} - \boldsymbol{P}_{Mx} \tag{17 a}$$

$$\boldsymbol{P}_{TMy} = \boldsymbol{P}_{Ty} - \boldsymbol{P}_{My} \tag{17 b}$$

Assuming that $\boldsymbol{R}_{TM}$ is the absolute distance between the missile and the target; closing velocity, $\boldsymbol{V}_c$ is defined as the negative change rate of the distance between the target and the missile.

Therefore;

$$V_c = -\acute{R}_{TM} \tag{18}$$

When the first derivative of Eq.16 is taken which is equal to Eq.18:

$$V_c = -\acute{R}_{TM} = -\frac{P_{TMx} \,.\, V_{TMx} + P_{TMy} \,.\, V_{TMy}}{R_{TM}} \tag{19}$$

where, relative velocity components are:

$$V_{TMx} = V_{Tx} - V_{Mx} \tag{20}$$

$$V_{TMy} = V_{Ty} - V_{My} \tag{21}$$

Considering the projections of R_{TM} on x and y axes, the line-of-sight angle, λ is:

$$\lambda = \arctan \frac{P_{TMy}}{P_{TMx}} \tag{22}$$

and the first derivative of λ is:

$$\dot{\lambda} = \frac{P_{TMx} \,.\, V_{TMy} - P_{TMy} \,.\, V_{TMx}}{R^2_{TM}} \tag{23}$$

when the variables in Eq.5 are replaced with the ones in Eq.19 and Eq.23, the magnitude of missile acceleration can be defined in terms of target-missile distance.

$$n_c = N' . \frac{-(R_{TMx} \,.\, V_{TMx} + R_{TMy} \,.\, V_{TMy})}{R_{TM}} \;.\; \frac{(R_{TMx} \,.\, V_{TMy} - R_{TMy} \,.\, V_{TMx})}{R^2_{TM}} \tag{24}$$

Since n_c is perpendicular to the instantaneous line-of-sight (LOS), missile acceleration components for x and y axes can be derived as follows:

$$a_{Mx} = -n_c \,.\, \sin\lambda \tag{25}$$

$$a_{My} = n_c \,.\, \cos\lambda \tag{26}$$

In practice, the missile is not launched on a collision triangle, since the expected intercept point is not known precisely. Any angular deviation of the missile from the collision triangle is called heading error and denoted ***HE***. Accordingly, initial missile velocity components can be expressed as:

$$V_{Mx}(0) = V_M \,.\, \cos\,(L + HE + \lambda) \tag{27}$$

$$V_{My}(0) = V_M \,.\, \sin\,(L + HE + \lambda) \tag{28}$$

Zero terms in the equations denote the initial conditions. The differential equations derived above are sufficient to model missile-target engagement in two-dimensions (2D) for True Proportional Navigation.

(2) Proportional Navigation Command Guidance

In command guidance a missile seeker does not exist. A source that is external to the missile, usually on the land or in a ship, both transmits and receives electromagnetic signals and their reflections to and from the target. Figure 5 shows the basic geometry of PN command guidance system.

As it can be seen in Fig. 5, R_M, is the range of the missile; R_T, is the range of the target; θ_M, is the sight angle of the missile; θ_T, is the sight angle of the target.

To derive line-of-sight information, the target and the missile position components must be computed firstly:

$$\tan \theta_T = \frac{P_{Ty}}{P_{Tx}} \tag{29}$$

the components of the distance vector from the external radar to the target:

$$P_{Tx} = R_T \,.\, \cos \theta_T \tag{30}$$

$$P_{Ty} = R_T \,.\, \sin \theta_T \tag{31}$$

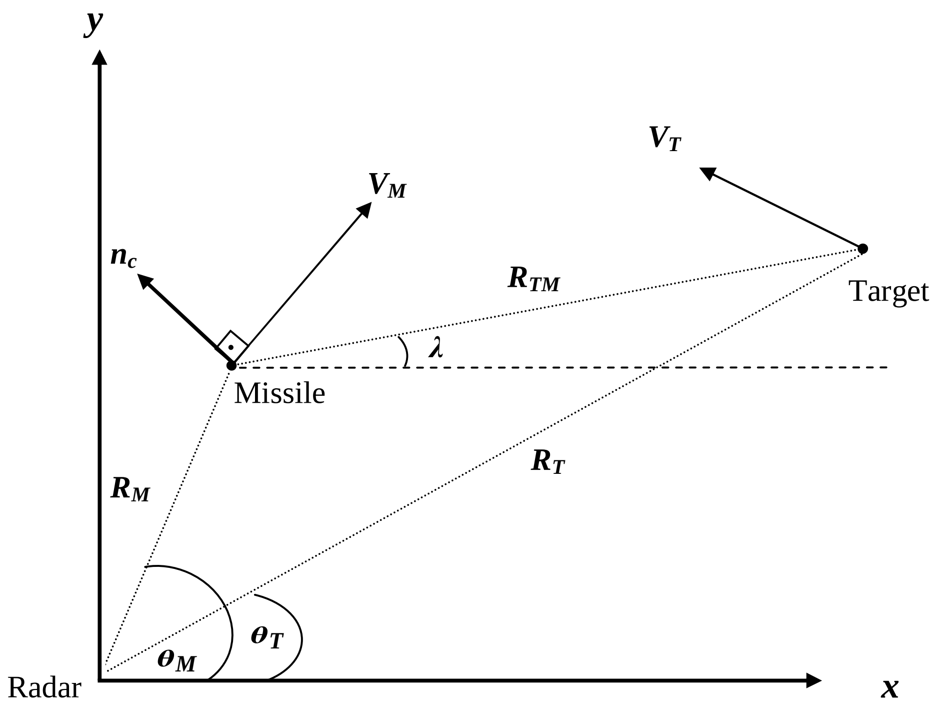

Figure 5   Fundamentals of Proportional Navigation Command Guidance

Similarly, the components of the range from the radar to the missile could be expressed as:

$$\tan \theta_M = \frac{P_{My}}{P_{Mx}} \tag{32}$$

and inertial components of the range from the radar to the missile in terms of the measurements:

$$P_{Mx} = R_M \cdot \cos \theta_M \tag{33}$$

$$P_{My} = R_M \cdot \sin \theta_M \tag{34}$$

The relative missile-target range components are:

$$P_{TMx} = R_{Tx} - R_{Mx} \tag{35}$$

$$P_{TMy} = R_{Ty} - R_{My} \tag{36}$$

And the line-of-sight angle can be expressed in terms of the relative range components as follows:

$$\boldsymbol{\lambda = arctan \frac{P_{TMy}}{P_{TMx}}} \tag{37}$$

Having derived Eq.29-Eq.37, other equations for the PN command guidance can be derived in the same way as done for the TPN in the previous section. In the command guidance process, unlike active homing processes, various range measurements are required to get the measurement of the LOS while in the active homing guidance, LOS angle information is available from the seeker avoiding additional range measurements. In command guidance, computed command is up-linked to the missile and it triggers relevant actions in the flight control system. However, in reality, guidance commands can not be implemented instantaneously by the flight control system or autopilot as there will be various lags within the guidance system. The limitation of command guidance is; as intercept takes place further away from the tracking radar, measurement accuracy and hence the guidance accuracy decreases.

(3) Augmented Proportional Navigation (APN)

Augmented PN (APN) is a modified form of PN to deal with target maneuvers. This guidance law is Proportional Navigation with an extra term to account for the maneuvering target. If the acceleration capability of the target is known exactly, it would be effective to use this type. The additional term related to target maneuver, required by the guidance law, appears as a feed-forward term in the formulation.

$$\boldsymbol{n_c = N' \cdot V_c \cdot \dot{\lambda} + (0{,}5 \cdot N' \cdot n_t)} \tag{38}$$

(4) Generalized True Proportional Navigation (GTPN)

In the Generalized True Proportional Navigation, computed acceleration command is not applied perpendicular to the line-of-sight but has a fixed angle, $\boldsymbol{\tau}$, relative to it. The engagement geometry for GTPN is given in Fig.6

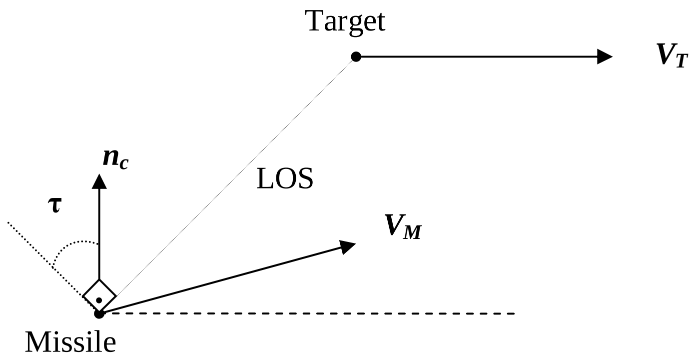

Figure 6 Generalized Proportional Navigation

(5) Pure Proportional Navigation (PPN)

Pure Proportional Navigation (PPN) consists of missile velocity referenced system while TPN, GTPN and APN use line-of-sight referenced systems. In the PPN, computed acceleration is applied perpendicular to the velocity vector of the missile. It has been shown that PPN approach is superior to TPN approach in terms of the performance metrics as given in [7]. However, the implementation of the PPN approach in homing missiles requires the exact value of the missile velocity, which is a time-varying magnitude and can be measured accurately only by using an extra navigation system onboard. On the other hand, TPN requires the closing velocity information which is taken easily from the Doppler radar. Hence, the applicability of TPN seems easier than the PPN [34]. Basic engagement geometry for the PPN scheme is given in Fig.7.

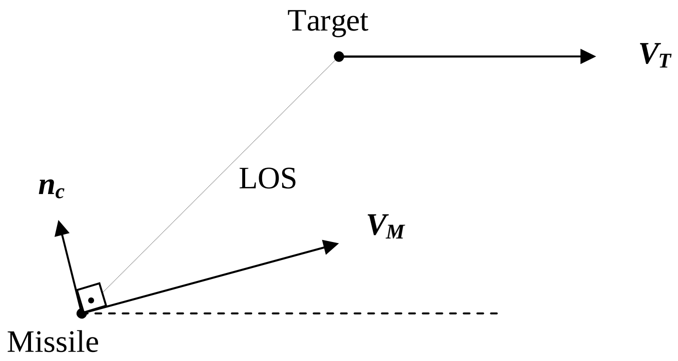

Figure 7 Pure Proportional Navigation

Until now, history and development of guided missiles, homing types, guidance concepts and guidance laws have been given and PN is explained in detail. In a real air engagement, there are various parameters act on a missile except the guidance law. One of the most essential parameter to be taken into account is aerodynamic state of the missile. After giving the guidance concepts of the missile in this chapter; aerodynamic concepts will be explained in the Chapter III.

III. MISSILE AERODYNAMICS

The ability of a tactical missile to maneuver depends upon its aerodynamic characteristics and the environmental properties in which missile flows through. In this chapter, fundamentals of aerodynamics is briefed first; followed by the aerodynamic forces act on a missile, derivation of aerodynamic coefficients, propulsion alternatives, thrust equations and issues related to the modeling of missile aerodynamics.

A. ATMOSPHERIC PROPERTIES

1. Air Density

Air density is the mass divided by the volume that the gas occupies. The air density is most dense at the sea level and is decreasing with the increasing altitude. The sea level standard value of air density, ***r*** is 1.229 kg/m^3. The change of air density is shown in Fig.8. Note that air density is one third of the sea level value at around 10 km.

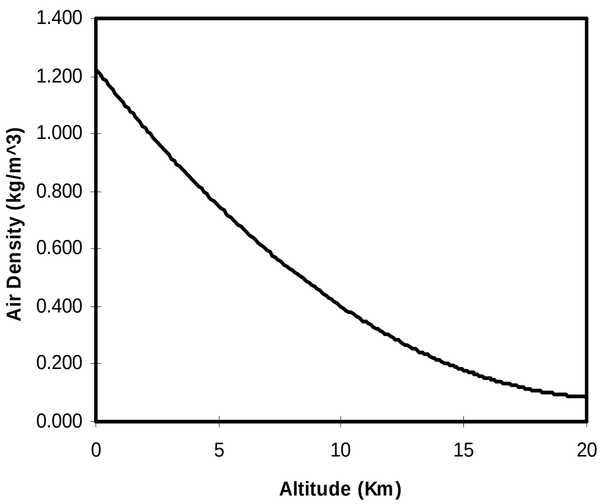

Figure 8 Change of Air Density With Respect to Altitude

2. Speed of Sound

Unfortunately there is no single value for the speed of sound. For example the speed of sound increases with an increase in temperature. However, air density and the speed of sound can be computed as functions of altitude for standard atmosphere models [35, 36]. Such models have been used in our models, as well.

3. Mach Number

The Mach number is used as an independent variable for stating aerodynamic measurement data and is defined as the ratio of the velocity of the vehicle and the speed of sound at current altitude.

$$\boldsymbol{M} = \frac{\boldsymbol{V}}{\boldsymbol{ss}} \tag{39}$$

where, ***V*** denotes the speed of the vehicle and ***ss*** denotes the speed of sound.

At high Mach numbers, significant changes in the air density happen because the airflow around the body of the missile suffers from the pressure changes. The change in the air density then increases the effects of pressure that produce aerodynamic forces. The changes in the magnitudes of aerodynamic forces are defined as compressibility effects.

Subsonic conditions occur for Mach numbers less than one, $\boldsymbol{M < 1}$. For the lowest subsonic conditions, compressibility can be ignored. As the speed of the missile approaches the speed of sound, the flight Mach number becomes very close to one, $\boldsymbol{M \approx 1}$, and the flow is said to be transonic. At some places on the object, the local speed exceeds the speed of sound. Compressibility effects are most important in transonic flows. In fact, the sound barrier is only an increase in the drag near sonic conditions because of compressibility effects. Because of the high drag associated with compressibility effects, aircrafts do not cruise about Mach 1.

Supersonic conditions occur for Mach numbers greater than one, $\boldsymbol{1 < M < 3}$. Compressibility effects are important for supersonic missile, and shock waves are generated by the surface of the object.

For high supersonic speeds; $3 < M < 5$, aerodynamic heating also becomes very important for aircraft and missile design. For speeds greater than five times the speed of sound, $M > 5$, the flow is said to be hypersonic. At these speeds, some of the object energy goes into exciting the chemical bonds which hold together the nitrogen and oxygen molecules of the air. At hypersonic speeds, the chemistry of the air must be considered when determining forces on the object.

In our study, an extended point mass missile model is assumed that achieves supersonic speeds. Mach number and the compressibility effects are used as aerodynamic state classifier of the missile since at supersonic speeds, derivations of the aerodynamic coefficients are computed not the same as at subsonic speeds. Considering that, in simulation tool VEGAS, Mach number is calculated instantaneously in the aero module.

B. AERODYNAMIC FORCES

Aerodynamic forces act on a missile as it flies through the air and are vector quantities having both a magnitude and a direction. The single aerodynamic force is broken into two components: the drag force is opposed to the direction of motion, while the lift force is perpendicular to the direction of motion and has an essential upward component.

Weight is another force on the missile due to the gravity, the direction of the weight is toward the center of the earth. The drag acts through the missile's center of pressure. Thrust is used to overcome drag and weight forces and the direction of thrust is on the missile velocity vector, V_M.

Aerodynamic forces are mechanical forces. They are generated by the interaction and contact of a solid body with a fluid, a liquid or a gas. Aerodynamic issues are important for a tactical guided missile because the entire flight path of the missile takes place in the atmosphere.

Equations of aerodynamic forces act on a missile such as thrust, drag and weight are explained with related physical missile parameters in the rest of this chapter.

1. Drag

Drag is an aerodynamic force that opposes motion of the missile through the air. Drag is a force and is therefore a vector quantity having both a magnitude and a direction. The drag force is usually characterized by a drag coefficient, C_D. Drag coefficient values can be obtained for missiles through wind tunnel tests and are usually provided as tabular data or making approximations.

a. Drag equation:

Drag formulation is given in Eq.40:

$$D = 0{,}5 \, . \, C_D \, . \, \rho . \, S_M \, . \, V_M^{\ 2} \tag{40}$$

where D is the drag force, C_D is the drag coefficient, ρ is air density, S_M is the reference area of the missile and V_M is the magnitude of missile velocity. For a missile, reference area is defined as cross sectional area of missile nose [37].

$$S_M = \pi \, .d^2 / 4 \tag{41}$$

The drag coefficient, C_D is a value used to model all of the complex dependencies of shape, inclination, and flow conditions on missile drag. C_D expresses the ratio of the drag force to the force produced by the dynamic pressure times the area. In a controlled environment, such as a wind tunnel, the velocity, density, and area could be set, hence a drag coefficient value could be derived. The choice of reference area will affect the actual numerical value of the drag coefficient. The drag could be predicted by using the drag equation, under a different set of velocity, density (altitude), and area conditions.

b. Derivation of Missile Drag Coefficient

The drag coefficient contains not only the complex dependencies of object shape, but also the effects of air viscosity and compressibility. At higher speeds, it becomes important to compute Mach numbers since at supersonic speeds, shock waves will be present in the flow field and it must be sure to account for the wave drag in the drag coefficient. Tactical missile airframe structure mainly occurs from two elements, body and the wings. When all the parameters mentioned above are included in, the total drag coefficient, C_D can be broken into two main components for the missile [37].

$$C_D = C_{D\ Body} + C_{D\ Wing} \tag{42}$$

(1) $C_{D\ Body}$

Firstly, the drag coefficient which comes from body structure of the missile is examined. Components of $C_{D\ Body}$ are:

$C_{D\ body\text{-}friction}$, skin friction drag coefficient,

$C_{D\ base\text{-}coast}$, base drag coefficient in coasting flight,

$C_{D\ base\text{-}powered}$, base drag coefficient in powered flight,

$C_{D\ body\text{-}wave}$, drag coefficient due to shock wave,

For supersonic missiles; drag is dominated by $C_{D\ wave}$ occurring on the nose of the missile, while $C_{D\ friction}$ and $C_{D\ base}$ are relatively small. The equations of these coefficients are:

$$C_{D\ body\text{-}friction} = 0.053 \cdot (l / d)\, [\, M / (q \cdot l)\,]^{0,2} \tag{43}$$

$$C_{D\ base\text{-}coast} = (0,25 / M), \qquad \text{if } (M>1) \tag{44}$$

$$C_{D\ base\text{-}coast} = (0.12+0.13M^2) \qquad \text{if } (M<1)$$

$$C_{D\ base\text{-}powered} = (1 - A_e / S_M)\,(0,25 / M) \qquad \text{if } (M>1) \tag{45}$$

$$C_{D\ base\text{-}powered} = (1 - A_e / S_M)\,(0.12+0.13M^2) \qquad \text{if } (M<1)$$

$$C_{D\ body\text{-}wave} = 3,6 / [\, (L_N/d).(M-1) + 3\,] \qquad \text{if } (M>1) \tag{46}$$

where, $\boldsymbol{l}$ is missile length, $\boldsymbol{d}$ is missile diameter, $\boldsymbol{M}$ is the mach number, $\boldsymbol{q}$ is dynamic pressure exerted on missile body, $\boldsymbol{A_e}$ is nozzle exit area, $\boldsymbol{S_M}$ is reference area of missile and $\boldsymbol{L_N}$ is nose length of the missile.

Considering Eq.43-Eq. 46, it can be seen that the wave drag, which is the dominant component of body drag, decreases with increasing nose fineness ratio and Mach number. Here, nose fineness ratio is defined as, length of missile nose divided by diameter of missile. For a nozzle exit area that is as large as the missile base area, the base drag could be assumed as zero during powered flight.

(2) $\boldsymbol{C_{D\ Wing}}$

The drag related with the wings, $\boldsymbol{C_{D\ Wing}}$, has two components as given in Eq.47: wing-wave and wing-skin friction drags.

$$\boldsymbol{C_{D\ Wing} = C_{D\ wing\text{-}wave} + C_{D\ wing\text{-}friction}} \tag{47}$$

Where, $\boldsymbol{C_{D\ wing\text{-}wave}} = 0$ if $\boldsymbol{M_{\Lambda LE}} \leq 1$

otherwise,

$$\boldsymbol{C_{D\ wing\text{-}wave}} = \frac{2\mathrm{n_w} \sin^2 \delta_{LE} \cos \Lambda_{LE} t_{mac} b}{\mathrm{S_M} \varepsilon \mathrm{M}^2{}_{\Lambda LE}} \cdot \left(\left(\frac{(\varepsilon+1)\mathrm{M}^2{}_{\Lambda LE}}{2} \right)^{\frac{\varepsilon}{\varepsilon-1}} \left(\frac{\varepsilon+1}{2\varepsilon \mathrm{M}^2{}_{\Lambda LE} - (\varepsilon-1)} \right)^{\frac{1}{\varepsilon-1}} - 1 \right) \tag{48}$$

and

$$\boldsymbol{C_{D\ wing\text{-}friction}} = \boldsymbol{n_w}\, [0{,}0133 / (\boldsymbol{q}\ .\boldsymbol{c_{mac}})^{0,2}]\ (\boldsymbol{2}\ .\ \boldsymbol{S_W / S_M}) \tag{49}$$

where, n_w is number of wings, S_W, is area of a wing in square feet, δ_{LE} is leading edge thickness angle, Λ_{LE} is leading edge sweep angle, t_{mac} is max thickness of mac, $M_{\Lambda LE} = M \cdot \cos \Lambda_{LE}$, q is dynamic pressure in *psf*, c_{mac} is length of mean aero chord in feet, b is wing span, ε is specific heat ratio =1.4

2. Thrust

The thrust force of a missile is a function of time defined by the characteristics of the rocket motor which moves a missile through the air. Thrust is used to overcome the drag and the weight of a missile and generated by the engines of the missile through a propulsion system. The propulsion system is in physical contact with propellant to produce thrust. Thrust is mostly generated through the reaction of accelerating a mass of gas. The engine works and accelerates the gas to the rear of the engine; the thrust is generated in the opposite direction from the accelerated gas.

The magnitude of the thrust depends on the amount of gas that is accelerated and on the difference in velocity of the gas through the engine.

The exit velocity is usually stated in terms of the specific impulse, I_{sp}, or the impulse produced per unit weight of propellant consumed. The specific impulse is related to the exit velocity by the Eq.50

$$V_e = I_{sp} \cdot g \tag{50}$$

where g is the acceleration due to gravity. The unit of I_{sp} is second. The specific impulse is a characteristic property of the propellant system.

There are several tactical missile propulsion alternatives. Figure 9 compares the efficiency of tactical missile propulsion alternatives across the specific impulse and the Mach number ranges of subsonic through supersonic. Turbojet, ramjet and solid rocket propulsion system alternatives are considered in this scheme.

Turbojet propulsion is suited for subsonic missiles, providing high efficiency against non-time-critical targets. Beyond Mach 2, expensive cooling is required to avoid exceeding the material temperature limit at the turbine inlet.

Ramjet is effective from Mach 2,5 to 5. Above Mach 5 the combustor material maximum temperature limits the achievable exit velocity and thrust. Deceleration to a subsonic velocity results in chemical dissociation of the air, which absorbs heat and negates a portion of the energy input of the combustor. It is also required to boost the missile to the ramjet velocity about Mach 2,5.

Solid rockets have an ability of providing thrust across the entire Mach number range. Besides, solid rockets have an advantage of much higher acceleration capability than the air-breathing propulsion. Operation ability at high altitudes is another advantage of this type [37].

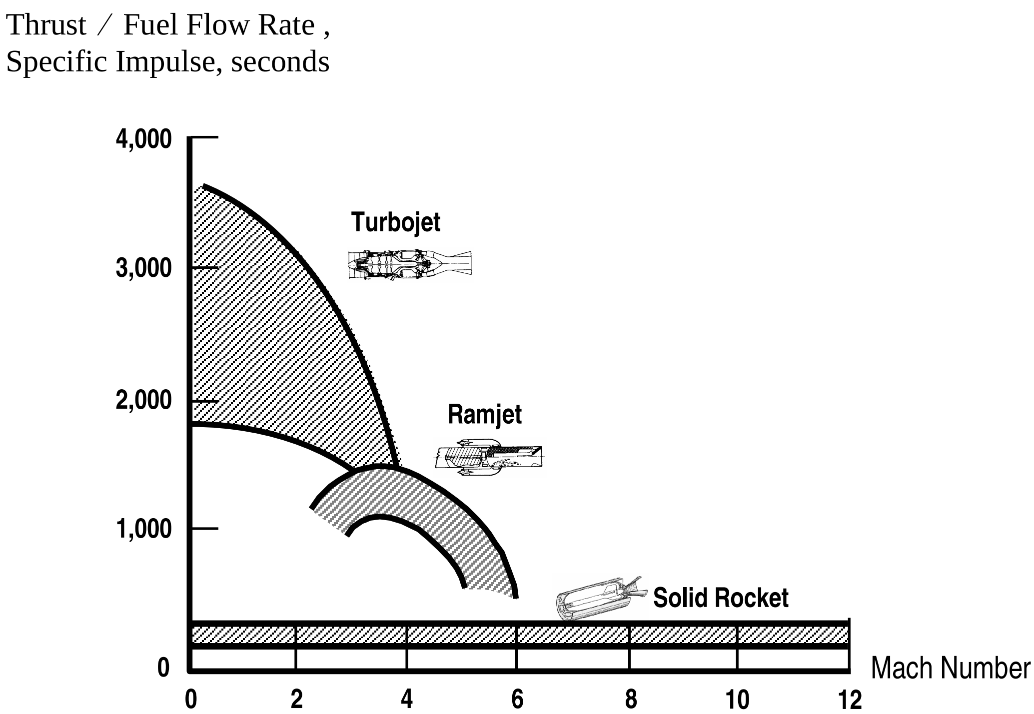

Figure 9 Tactical Missile Propulsion Alternatives [37]

Comparison of tactical missile propulsion alternatives based on acceleration capability is shown in Figure 10. The comparison is defined as a function of Mach number and maximum thrust-to-weight ratio. It is clear that the highest thrust-to-weight ratio belongs to the solid rocket propulsion system.

The reason is, higher exit velocity, independence of the exit velocity from that of the free stream velocity and the capability of higher mass flow rate.

Turbojets and ramjets produce thrust only if the exit velocity is greater then the free stream velocity. The maximum velocity of an air-breathing missile is less than the exit velocity

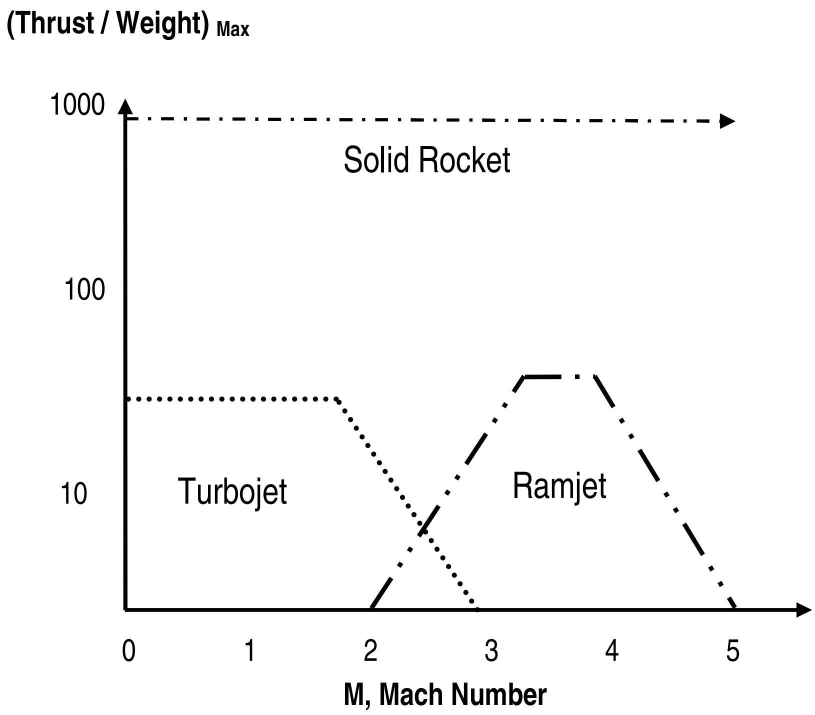

.

Figure 10 Acceleration Capabilities of Tactical Missile Propulsion Systems [37]

Maximum thrust for these propulsion systems are given in Eq.51 and Eq.52.

The maximum thrust for Turbojet and Ramjet is:

$$\boldsymbol{T_M} = (\boldsymbol{\pi} / 4)\, \boldsymbol{d^2}\, \boldsymbol{\rho_\infty V_\infty^2}\, [(\boldsymbol{V_e} / \boldsymbol{V_\infty}) - 1] \tag{51}$$

The maximum thrust for Solid Rocket is:

$$\boldsymbol{T_M} = 2\, \boldsymbol{P_C A_t} = \dot{\boldsymbol{m}} \,.\boldsymbol{V_e} \tag{52}$$

where, $\boldsymbol{P_C}$ is chamber pressure, $\boldsymbol{V_\infty}$ is free stream velocity, $\boldsymbol{A_t}$ is nozzle throat area, $\boldsymbol{\rho_\infty}$ is free stream density, $\boldsymbol{d}$ is missile diameter, $\dot{\boldsymbol{m}}$ is mass flow rate, $\boldsymbol{V_e}$ is nozzle exit velocity.

$\boldsymbol{V_e}$ ~ 610 meters /sec. for Turbojet,

$\boldsymbol{V_e}$ ~ 1372 meters /sec. for Ramjet,

$\boldsymbol{V_e}$ ~ 1830 meters /sec. for Solid Rocket [37].

3. Weight

Weight is one of the main forces affecting the aerodynamic condition of the missile. In mathematical formulation, the weight is:

$$\boldsymbol{W} = \boldsymbol{m} \,.\, \boldsymbol{g} \tag{53}$$

Where, $\boldsymbol{m}$ is the mass and $\boldsymbol{g}$ is the gravitational force. Mass can be considered fixed or it may depend on the fuel consumption, which for a missile is typically a fixed function of time, and the direction of the gravitational force, $\boldsymbol{g}$ is considered as towards center of the earth.

In this chapter, missile aerodynamic topics are discussed. Atmospheric properties; equations of aerodynamic forces acting on a missile such as thrust, drag and weight, the derivation of missile drag coefficients at different Mach numbers, missile propulsion alternatives and the derivation of thrust force are explained in detail with related physical missile parameters. In performance evaluation of our new guidance law approach, aerodynamic issues that affect the motion of missile are computed as to the formulations given here.

IV. THE THREE PLANE APPROACH (TPA) FOR 3D TRUE PROPORTIONAL NAVIGATION

Keeping the essentials of two-dimensional TPN approach explained in Chapter II.B.3.d.(1) in mind, Three Plane Approach (TPA) has been developed and is explained in detail in this chapter. In the TPA; three dimensional (3D) engagement space is projected onto three perpendicular planes: S_{xy}, S_{xz} and S_{yz}. (Figure 11)

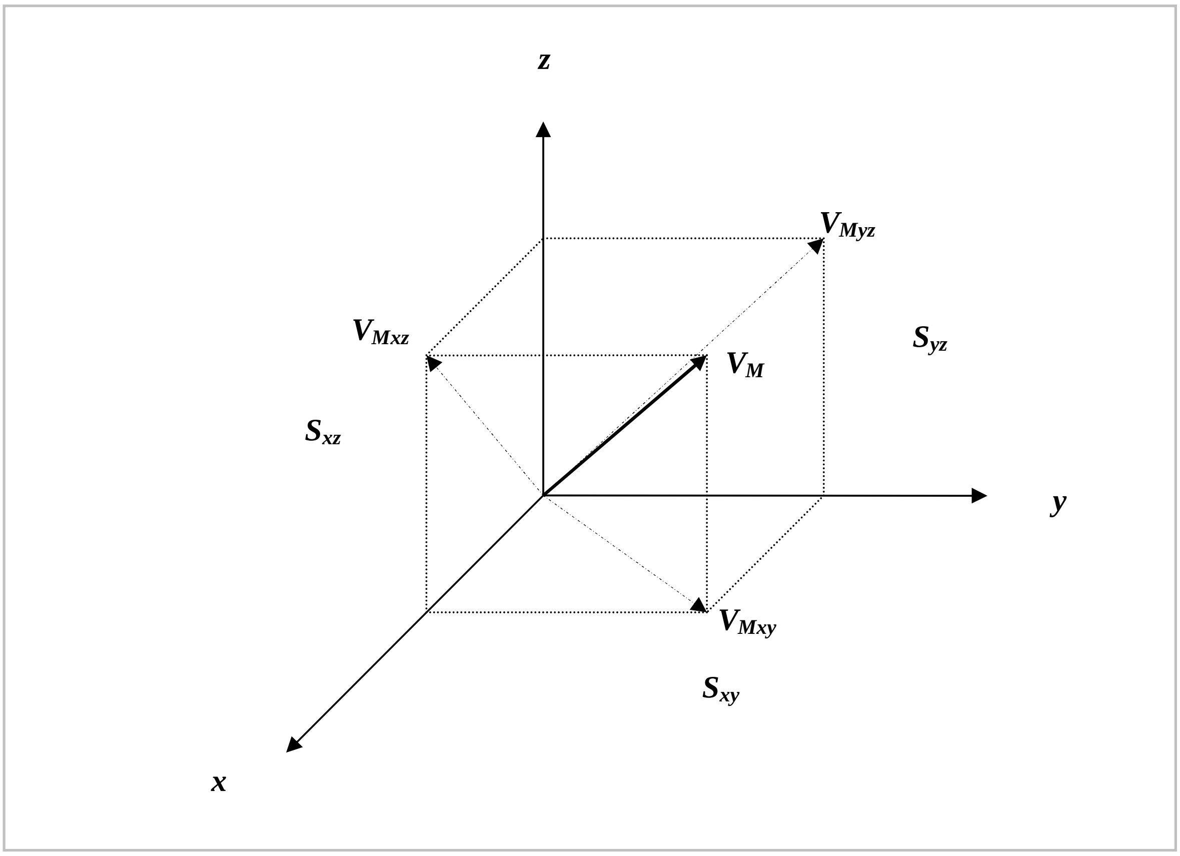

Figure 11 Projections of Missile Velocity Vector on to Three Planes

The projections of missile velocity vector on to the planes are shown in Fig.11. In a pursuit-evasion scenario, there are two main vectors to deal with: target and missile velocity vectors.

It is assumed that the missile and the target are point mass and having the velocity vectors $\boldsymbol{V_T}$, $\boldsymbol{V_M}$ respectively. The projection of such two point masses' relative motion geometry to $\boldsymbol{S_{xy}}$, $\boldsymbol{S_{xz}}$ and $\boldsymbol{S_{yz}}$ planes are shown in Fig. 12 (a),(b),(c).

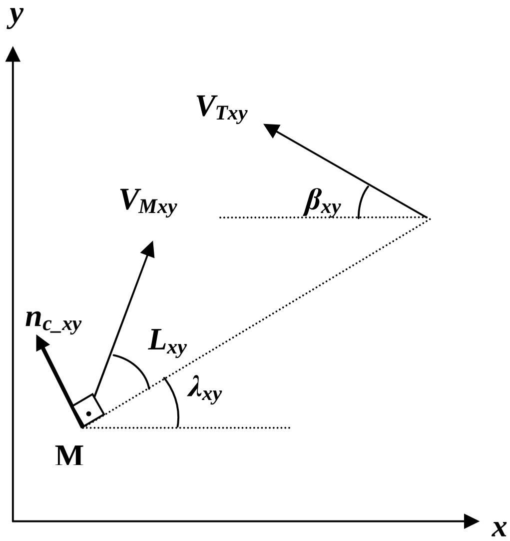

(a) S_{xy} Plane

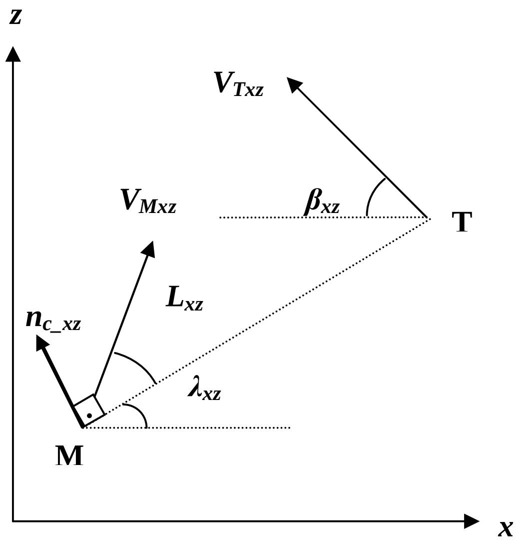

(b) S_{xz} Plane

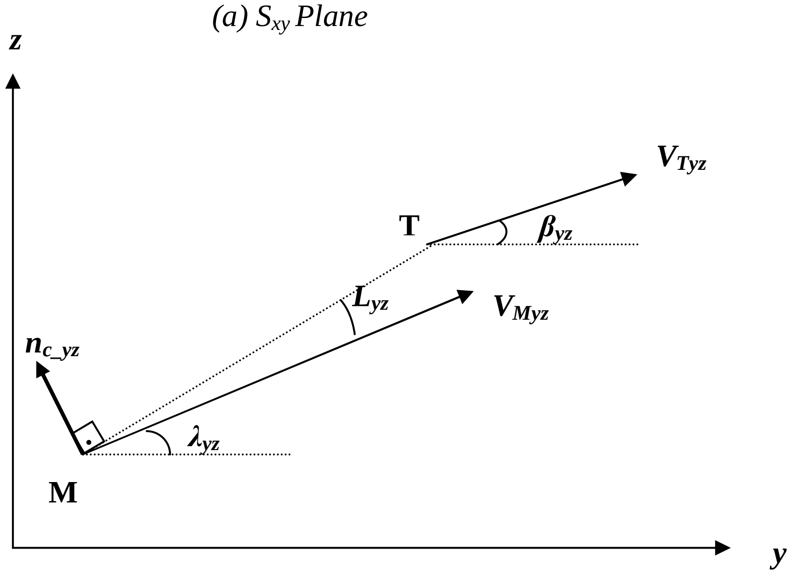

(c) S_{yz} Plane

Figure 12 The Projections of Target's and Missile's Relative Motion onto $\boldsymbol{S_{xy}}$, $\boldsymbol{S_{xz}}$ and $\boldsymbol{S_{yz}}$ Planes

Our approach to solve guidance problem in 3D space is to project 3D geometry onto 3 perpendicular planes such as, $\boldsymbol{S_{xy}}$, $\boldsymbol{S_{xz}}$ and $\boldsymbol{S_{yz}}$; to solve the problem in each plane independently for two-dimensional True Proportional Navigation (TPN) and to produce a 3D solution by combining these 2D solutions.

Considering Fig.11 and Fig.12, the components of 2D solutions and equations to combine those to provide 3D solutions are derived as follows:

The distance between the target and the missile is:

$$\boldsymbol{R_{TM}} = \sqrt{\boldsymbol{P^2}_{TMx} + \boldsymbol{P^2}_{TMy} + \boldsymbol{P^2}_{TMz}} \tag{54}$$

The line of sight (LOS) angles:

$$\lambda_{xy} = \arctan \frac{P_{TMy}}{P_{TMx}} \tag{55 a}$$

$$\lambda_{xz} = \arctan \frac{P_{TMz}}{P_{TMx}} \tag{55 b}$$

$$\lambda_{yz} = \arctan \frac{P_{TMz}}{P_{TMy}} \tag{55 c}$$

Target flight-path angles:

$$\beta_{xy} = \arctan \frac{\Delta P_{Ty}}{\Delta P_{Tx}} \tag{56 a}$$

$$\beta_{xz} = \arctan \frac{\Delta P_{Tz}}{\Delta P_{Tx}} \tag{56 b}$$

$$\beta_{yz} = \arctan \frac{\Delta P_{Tz}}{\Delta P_{Ty}} \tag{56 c}$$

Projection of target velocity vector onto $\boldsymbol{S_{xy}}$, $\boldsymbol{S_{xz}}$ and $\boldsymbol{S_{yz}}$ planes:

$$V_{Txy} = \sqrt{V^2_{Tx} + V^2_{Ty}} \tag{57 a}$$

$$V_{Txz} = \sqrt{V^2_{Tx} + V^2_{Tz}} \tag{57 b}$$

$$V_{Tyz} = \sqrt{V^2_{Ty} + V^2_{Tz}} \tag{57 c}$$

Missile lead angles, $\boldsymbol{L_{xy}}$, $\boldsymbol{L_{xz}}$ and $\boldsymbol{L_{yz}}$ for each plane (i.e., $\boldsymbol{S_{xy}}$, $\boldsymbol{S_{xz}}$, $\boldsymbol{S_{yz}}$) have to be computed considering Eq.54-Eq.57 c. In order to find the current leading angles for all possible engagement schemes:

$$L_{xy} = \arcsin \frac{V_{Txy} \,.\, \sin(\beta_{xy} + \lambda_{xy})}{V_M} \tag{58 a}$$

$$L_{xz} = \arcsin \frac{V_{Txz} \,.\, \sin(\beta_{xz} + \lambda_{xz})}{V_M} \tag{58 b}$$

$$L_{yz} = \arcsin \frac{V_{Tyz} \,.\, \sin(\beta_{yz} + \lambda_{yz})}{V_M} \tag{58 c}$$

It can be seen from Eq.5 and Eq.24 that to produce the required acceleration commands for each plane; their closing velocity ($\boldsymbol{V_c}$) and line of sight (LOS) change rate ($\dot{\lambda}$) values must be computed. From Eq.55 (a)-(c); change rates of LOS angles can be derived as:

$$\dot{\lambda}_{xy} = \frac{P_{TMx} V_{TMy} - P_{TMy} V_{TMx}}{P^2_{TMx} + P^2_{TMy}} \tag{59 a}$$

$$\dot{\lambda}_{xz} = \frac{P_{TMx} V_{TMz} - P_{TMz} V_{TMx}}{P^2_{TMx} + P^2_{TMz}} \tag{59 b}$$

$$\dot{\lambda}_{yz} = \frac{P_{TMy} V_{TMz} - P_{TMz} V_{TMy}}{P^2_{TMy} + P^2_{TMz}} \tag{59 c}$$

To compute the closing velocities(V_{Cxy}, V_{Cxz}, V_{Cyz}) for each plane; P_{TMxy}, P_{TMxz}, P_{TMyz} values must be differentiated just like in Eq.19, thus,

$$V_{Cxy} = -\frac{P_{TMx}.V_{TMx} + P_{TMy}.V_{TMy}}{(P^2_{TMx} + P^2_{TMy})^{1/2}} \tag{60 a}$$

$$V_{Cxz} = -\frac{P_{TMx}.V_{TMx} + P_{TMz}.V_{TMz}}{(P^2_{TMx} + P^2_{TMz})^{1/2}} \tag{60 b}$$

$$V_{Cyz} = -\frac{P_{TMy}.V_{TMy} + P_{TMz}.V_{TMz}}{(P^2_{TMy} + P^2_{TMz})^{1/2}} \tag{60 c}$$

where, relative velocity components are:

$$V_{TMx} = V_{Tx} - V_{Mx} \tag{61 a}$$

$$V_{TMy} = V_{Ty} - V_{My} \tag{61 b}$$

$$V_{TMz} = V_{Tz} - V_{Mz} \tag{61 c}$$

Hence,

$$n_{c\_xy} = N' . V_{Cxy} . \dot{\lambda}_{xy} \tag{62 a}$$

$$n_{c\_xz} = N' . V_{Cxz} . \dot{\lambda}_{xz} \tag{62 b}$$

$$n_{c\_yz} = N' . V_{Cyz} . \dot{\lambda}_{yz} \tag{62 c}$$

acceleration commands for S_{xy}, S_{xz} and S_{yz} planes are derived.

Missile acceleration components (a_{Mx}, a_{My}, a_{Mz}) for x, y and z axis can be computed by combining two components sharing the same axis. Fig.12 indicates that one axe' acceleration component is interacted by 2 planes' acceleration commands. By the help of trigonometric relationships, unified missile acceleration components of axes x, y and z can be founded as below:

$$a_{Mx} = - n_{c\_xy} . \sin \lambda_{xy} - n_{c\_xz} . \sin \lambda_{xz} \tag{63 a}$$

$$a_{My} = n_{c\_xy} . \cos \lambda_{xy} - n_{c\_yz} . \sin \lambda_{yz} \tag{63 b}$$

$$a_{Mz} = n_{c\_xz} . \cos \lambda_{xz} + n_{c\_yz} . \cos \lambda_{yz} \tag{63 c}$$

In the literature, [23, 38, 39, 40] while implementing the acceleration commands as control variables in equations of motion, they are broken into vertical and horizontal components, named as a_{pitch} and a_{yaw}.

The vertical acceleration component, a_{pitch} is directed perpendicular to the velocity vector of the missile and upwards, and the horizontal component, a_{yaw} is perpendicular to both the velocity vector and the vertical acceleration component. The suggested vertical and horizontal accelerations generated by Proportional Navigation are defined as:

$$a_{pitch} = N' \,.\, V_c \,.\, \dot{\lambda}_{pitch} + g \,.\, \cos \gamma_M \tag{64}$$

$$a_{yaw} = N' \,.\, V_c \,.\, \dot{\lambda}_{yaw} \tag{65}$$

where, γ_M is flight path angle between the velocity vector and its projection onto the xy plane; $\dot{\lambda}_{pitch}$ and $\dot{\lambda}_{yaw}$ are the line-of-sight rates (LOSR) for relative vertical and horizontal motion respectively. These acceleration commands can not exceed the maximum achievable acceleration limits of the missile imposed by the structural limits.

In our study, vertical and horizontal components of acceleration commands, a_{pitch} and a_{yaw} are computed in a different method. As seen on Fig. 13 and Fig.14, vertical component of missile acceleration command can be derived as:

$$a_{pitch} = a_{Mz} \,.\, \cos \gamma_M + g \,.\, \cos \gamma_M \tag{66}$$

and the lateral component of missile acceleration command:

$$a_{yaw} = a_{My} \,.\, \sin \left(\frac{\pi}{2} - \chi_M\right) - a_{Mx} \,.\, \sin \chi_M \tag{67}$$

These acceleration components, a_{pitch} and a_{yaw}, will be used as control variables of the missile in the equations of motion.

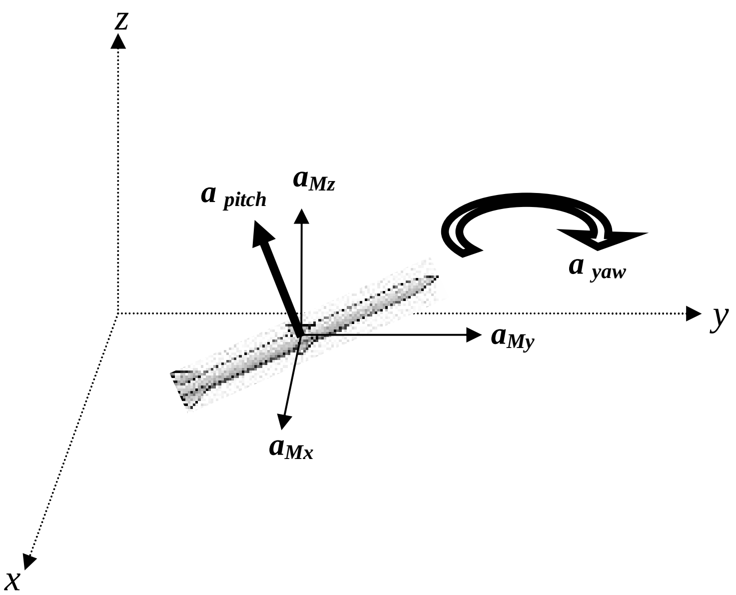

Figure 13 Components of Missile Acceleration Commands in 3D Environment

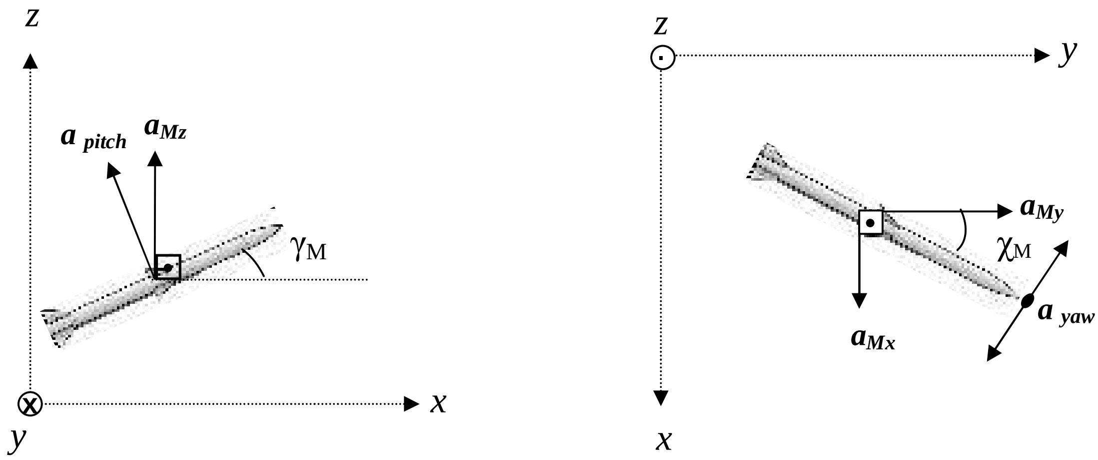

*Figure 14   Projections of Missile Acceleration Commands onto **xz** and **xy** Planes*

In this chapter; Three Plane Approach (TPA) for 3D True Proportional Navigation has been explained.

To summarize TPA, to solve the guidance problem; 3D engagement space geometry is projected onto 3 perpendicular planes such as, $\boldsymbol{S_{xy}}$, $\boldsymbol{S_{xz}}$ and $\boldsymbol{S_{yz}}$. Guidance problem is solved in each plane independently for two-dimensional True Proportional Navigation (TPN); acceleration commands are generated for each plane, and a 3D solution is produced by combining these 2D solutions.

In Chapter VI, TPA is used as missile guidance law and effectiveness of TPA against targets employing evasive maneuvers is examined within aerodynamic limitations.

V. VISUAL END-GAME SIMULATION: VEGAS

In this thesis, the missile and the guidance history, mostly used guidance laws, analytic solution of TPN and aerodynamic forces on a missile are examined respectively. After having this background, a new 3D guidance law approach is developed named Three Plane Approach (TPA), based on TPN. This approach is developed for active homing air-to-air or surface-to-air missiles' terminal phase in an encounter.

In another thesis [1], Akdağ studied comparative evaluation of basic fighter maneuvers against PN guided missiles. In this work, beside the mostly used basic evasive maneuvers, flight dynamics of high acceleration capability fighter aircrafts are investigated.

From the missile point of view; a target model is required to evaluate the effectiveness of new guidance law; while, a guided missile model is required to evaluate the effectiveness of the evasive maneuvers from the fighter aircraft point of view.

To provide a solution to these requirements, that is, to evaluate the performance of guidance law proposed in this thesis; a simulation sofware, VEGAS is implemented, in which the missile and the target are independent modules. Hence it would be possible to evaluate the effectiveness of both sides.

This simulation software is named as, Visual End-Game Simulation, VEGAS. The last seconds of the encounter is also called End-Game. The VEGAS software is implemented in Visual C++ programming language using OpenGL library. Different modules of this simulator have been designed, developed and implemented by Moran and Akdağ [1] as parts and partials of their master thesis projects.

The terminal phase of the encounter between the missile and the aircraft is considered in the VEGAS. These last seconds of the engagement are the most important period since its success or failure determines the success or failure of the entire mission.

Since the scenarios of this simulation tool starts at the beginning of the terminal phase, the missile and the aircraft are assumed to have initial velocities and some kilometers from each other. All the aerodynamic and physical parameters of both missile and target aircraft are included in VEGAS. It is realized that the developed guidance approach works effectively against high-g capacity fighter aircrafts. The results are illustrated by both analytical and 3D visual demonstrations for the user to deeply observe the terminal phase of the engagement.

A. DESIGN FEATURES

The VEGAS is comprised of five basic modules:

- Main
- Evader
- Pursuer
- Radar
- Aero

The overall flow chart of Visual End-Game Simulation is given in Fig.15. As seen on the chart, the simulation steps are as follows:

1. Target makes a step of evasion maneuver in 3D environment with respect to aerodynamic considerations.

2. Missile takes the position data of target from the “radar” module.

3. Missile guidance law generates the acceleration commands with respect to the engagement geometry.

4. By using the parameters coming from “aero” module, aerodynamic forces such as drag, thrust, weight are computed, limits are controlled. Translational movement in 3D is derived from equations of motion with all these values.

These steps are repeated while the range between target and missile is larger than the capture radius R_C and the target is in the missile seeker cone.

Since VEGAS is a discrete-time simulation, motions of the missile and the target are performed in fixed time steps. The size of time step is assumed equal to the missile's guidance system time constant which is the total lag of guidance system.

1. Main Module

"main" module could be assumed as referee function and the manager of the simulation. It starts and ends the simulation according to the user-chosen conditions and is responsible for the visualization. It firstly initials the simulation by getting from the user the variables such as:

- initial positions of pursuer and evader on 3D environment,
- initial velocities of pursuer and evader at the beginning of the terminal phase,
- initial heading and flight path angles of pursuer and evader.

By getting these initial conditions, all the possible scenarios can be generated in 3D space. Capture radius, $\boldsymbol{R_C}$, is set in advance and considered as a success metric of the missile. After setting the initial conditions, the simulation begins and continues by calling the "evader" and the "pursuer" modules respectively, while the target in the field of missile seeker cone and the range between the "pursuer" and "evader" is greater than the capture radius, $\boldsymbol{R_C}$. Success or failure is decided with respect to the target's being in the missile's seeker cone and the miss distance. If the miss distance, that is closest range between the pursuer and the evader in entire flight, is greater than the capture radius, $\boldsymbol{R_C}$, or target is out of the missile's seeker cone it is assumed failure. After the simulation ends with success or failure result, the trajectory traces of both vehicle can be seen from any view that user selected.

Also the visual settings are located in "main" module. VEGAS is designed in such a way that the user has the ability of choosing the camera location and its orientation. That feature enables the user to observe the engagement from all the possible views.

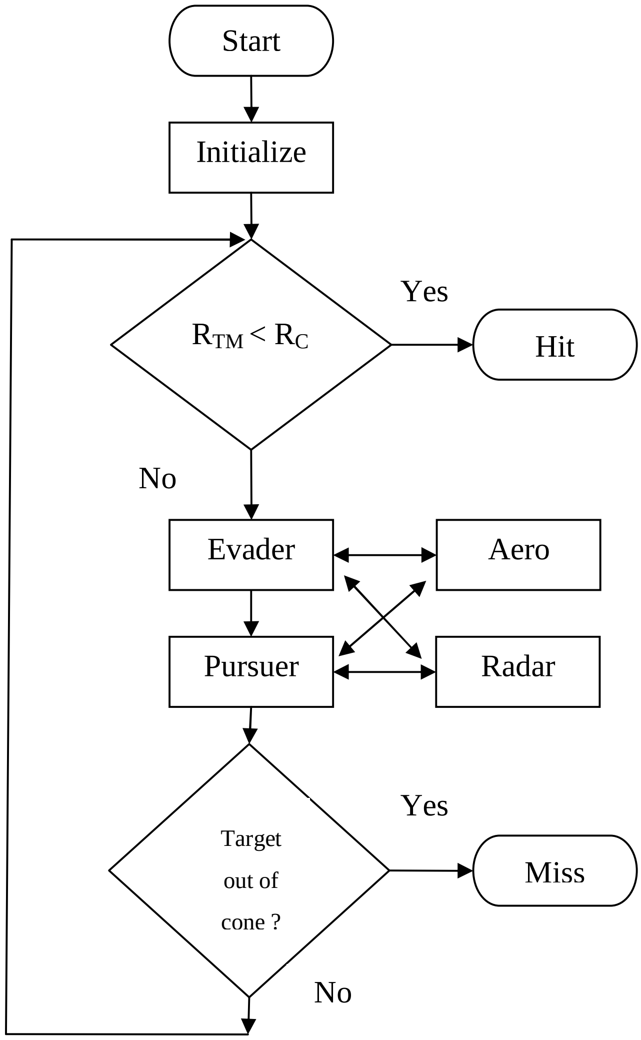

Figure 15 Flow Chart of Visual End-Game Simulation

2. Radar Module

The function of “radar” module is giving the current coordinates of target and missile to each other. This module is used by both “evader” and “pursuer” modules. When the “evader” completed the evasive maneuver in fixed time-step of the simulation, it sends its ***id*** and current ***x, y, z*** coordinates to the “radar” module.

When it is pursuer's turn; "pursuer" module sends its ***id*** and current location to the "radar" module and acquires the target coordinates in ***x, y, z*** axis.

Although "radar" module produces perfect map of engagement space upon the requests from "pursuer" and "evader", the module structure is designed to support producing signal superimposed with noise.

3. Aero Module

"aero" is the mutual module that is used by both "pursuer" and "evader". It obtains the information of air density and Mach number, which are related with the altitude and the velocity that vehicles have instantaneously.

4. Evader Module

The evasive maneuvers and flight dynamics of combat aircraft are included into the "evader" module. Alternatives of basic fighter aircraft maneuvers and related aerodynamics are implemented in this module. The user can select the maneuver which target aircraft will carry out in the simulation. The "evader" module is organized by Akdağ [1] and detailed information about evader can be found in this study.

5. Pursuer Module

The issues that effect the missile maneuver such as derivation of acceleration commands, aerodynamic forces, missile characteristics etc., are included into "pursuer" module of the VEGAS. The fundamentals of mentioned issues are discussed in the Section II, III and IV.

"pursuer" module is in relation with "radar" and "aero" modules. "pursuer" obtains the target information from "radar" module. After computing acceleration commands that will be implemented by autopilot or the control section of the missile, "pursuer" sends its own altitude and velocity as input parameters and gets the results such as Mach number and air density as return values from "aero" module.

The equations of motion are employed with respect to the aerodynamic forces on the missile. Pursuer module is shown in Fig.16 in detail.

When the "pursuer" module is called by "main" module, some calculations are done. These are:

- target location is acquired from "radar" module,
- target velocity components of ***x, y*** and ***z*** axis,
- relative position vectors for ***x, y*** and ***z*** axis,
- line-of-sight angles (LOS) for ***xy, xz*** and ***yz*** planes,
- target flight-path angles for ***xy, xz*** and ***yz*** planes,
- in first step, missile leading angles and initial velocity components,
- relative and closing velocities for ***xy, xz*** and ***yz*** planes,
- line-of-sight change rates for ***xy, xz*** and ***yz*** planes,
- acceleration commands for ***xy, xz*** and ***yz*** planes,
- acceleration commands for ***x, y*** and ***z*** axis,
- vertical and lateral components of acceleration, a_{pitch} and a_{yaw}, as control variables
- density and Mach number for instant conditions of the missile
- drag coefficient and drag force,
- thrust equation as a function of time,
- equations of motion, extended point mass missile model translational movement

One step of missile maneuver is ended after terms above are calculated. In the computation of the missile control variables, a_{pitch} and a_{yaw}, acceleration limitations (30-g) are included to make a realistic missile model.

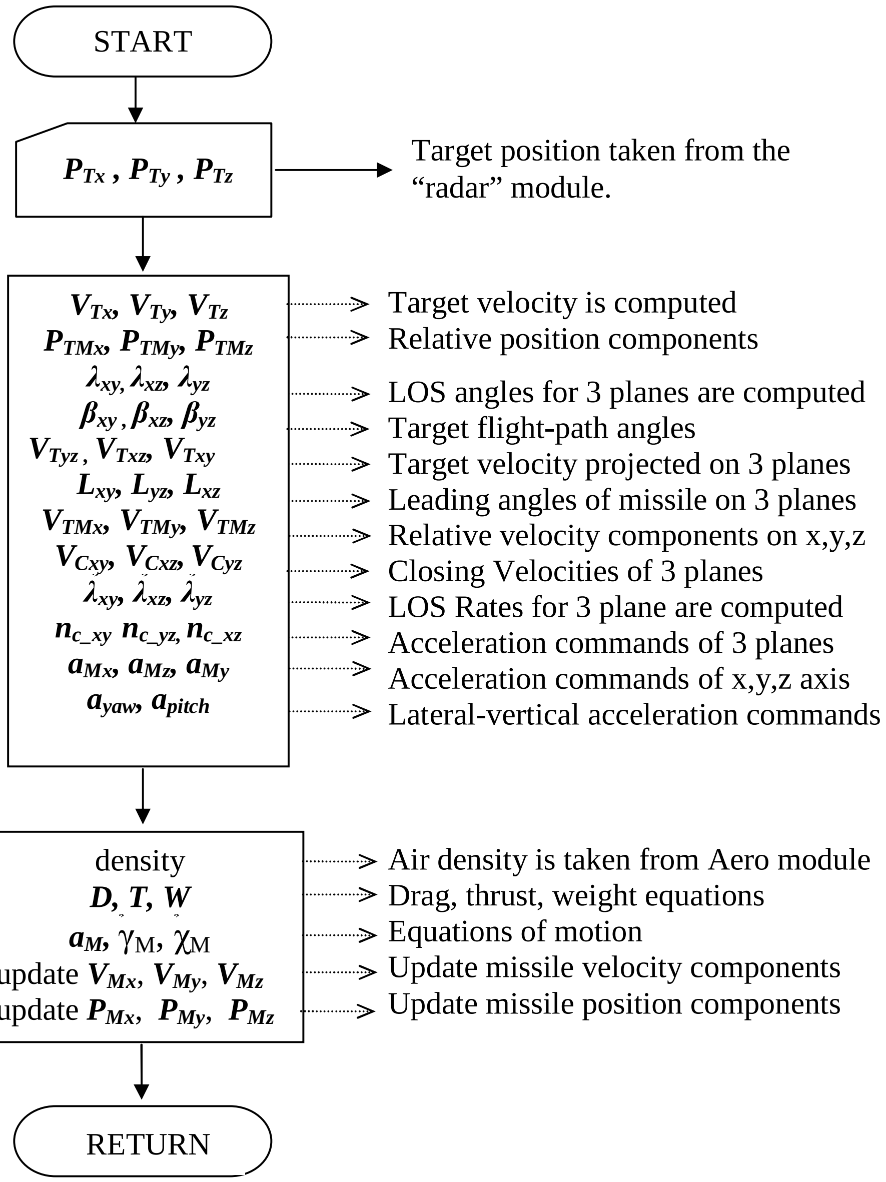

Figure 16 Flow Chart of the "Pursuer" Module

VI. PERFORMANCE EVALUATION

In this chapter, a missile guided with the TPA approach presented in Chapter IV and a target fighter aircraft are considered. The air combat between the fighter aircraft employing evasive maneuvers and the missile guided by proposed approach to intercept this aircraft is examined. VEGAS, described in the previous section, is used as the discrete-time simulation software.

The time constants of both missile and aircraft are assumed as 0.1 second. Although, the guidance system dynamics are quite significant in practice and in the tactical missiles; in this thesis, the time constants of guidance dynamics are assumed negligibly small compared to the dynamics of translational motion.

Aircraft and missile models used in the simulations are based on the extended point mass assumptions. The earth is assumed flat because the relative distance between the missile and target is short in the terminal guidance phase and thus the curvature of earth is considered not to be able to affect the dynamics of the flight. The velocity vector, reference line of the vehicle, the thrust and drag forces are all assumed parallel. (Fig.17) Also wind is ignored in the missile and target models hence the side-slip angle is assumed to be zero. The dynamic model of the missile and the aircraft and their guidance dynamics are presented below. These assumptions are associated with Miele [41]. Missile and target models that used in our simulations are given below.

A. MISSILE MODEL

The evaluation of the missile flight trajectory requires consideration of degrees of freedom (DOF) to be simulated. The simplest and the acceptable model for the conceptual design of the high speed missiles, one degree-of-freedom is considered to model the missile. One degree-of-freedom requires only thrust, weight and drag forces of the missile [37].

In one degree-of-freedom modeling, heading angle and flight path angles are used as state variables. The position of the missile in the three-dimensional (3D) space is defined by three state variables, which are coordinates ***x*** and ***y*** range and altitude ***z***.

The missile is directly controlled with commanded accelerations $\boldsymbol{a_{pitch}}$ and $\boldsymbol{a_{yaw}}$, those are generated by the guidance law developed in Section IV.

Missile employs STT (Skid-to-Turn) maneuvering method to implement these acceleration commands. STT maneuvering is commanded along the line-of-sight (LOS) of the seeker without rolling and is generally preferred due to its fast response to the acceleration commands [37].

The angle of attack and the bank angle are assumed to be zero. The Euler angles and the directions of the aerodynamic forces on a missile are shown in Fig-17.

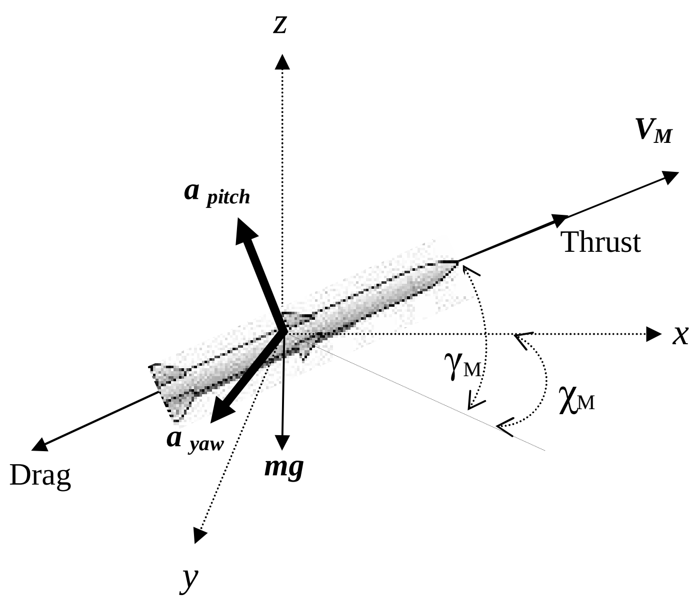

Figure 17 Angle and Force Definitions of Three-dimensional Missile Model

Equations of motion with respect to Euler angles are as follows:

$$V_{Mx} = V_M \,.\, \cos \gamma_M \cos \chi_M \tag{68}$$

$$V_{My} = V_M \,.\, \cos \gamma_M \sin \chi_M \tag{69}$$

$$V_{Mz} = V_M \,.\, \sin \gamma_M \tag{70}$$

$$a_M = \frac{T_M - D_M}{m_M} - g \,.\, \sin \gamma_M + a_{Mx} \,.\, \cos \chi_M + a_{My} \cos (90° - \chi_M) + a_{Mz} \,.\, \sin \gamma_M \tag{71}$$

$$\dot{\gamma}_M = \frac{a_{pitch} - g \cos \gamma_M}{V_M} \tag{72}$$

$$\dot{\chi}_M = \frac{a_{yaw}}{V_M \cos \gamma_M} \tag{73}$$

where,

V_{Mx}, V_{My} and V_{Mz} are the components of missile velocity on axis x, y and z;

a_M, total acceleration of missile;

γ_M, missile flight path angle, is the angle between the velocity vector and its projection onto the xy plane;

χ_M, heading angle, is the angle between the projection of the velocity vector onto the xy plane and the x axe;

T_M is thrust force of the missile; D_M is drag force on the missile;

m_M is mass of the missile; g is the gravitational force.

The mass of the vehicle and its change due to fuel consumption are also included into simulation as a state variable. The propellant mass at the terminal phase is assumed equal to 30 kg. and change rate of propellant mass, so the total mass rate of the missile during this period is:

$$\dot{m}_M = -3 \text{ kg/sec.} \tag{74}$$

Parameter	**Value**
Missile Length, l	3,66 m
Diameter, d	0,17 m
L_N / d, nose fineness ratio	3
Mass of the missile, m_M	100 kg.
Thrust force, T	5490 N
Weight of propellant at the beginning of terminal phase	30 kg.
Propellant flow rate, $\dot{m}_M$	− 3 kg / sec.
Burn time, t_B	10 sec.
Reference Area, S_M	0,026 m^2
Maximum acceleration limit	30 g
Nozzle exit area, A_e	0.0052 m^2
n_w, number of wings	2
ε, specific heat ratio	1.4
δ_{LE}, leading edge thickness angle	10 deg.
Λ_{LE} , leading edge sweep angle	45 deg.
t_{mac} , max thickness of mac	1,48 cm
b, span	81,78cm
c_{mac}, length of mean aero chord in ft	33,79 cm

Table 1 Missile Model Specifications

Thrust force of our missile model is the function of the time during flight. From Eq.52, thrust force during 10 seconds of the terminal phase is equal to:

$$T_M = \dot{m}\, V_e = -3 \text{ kg/sec} . 1830 \text{ m/sec} = 5490 \text{ N}$$

From Eq.40, the drag force of our missile model is:

$$D = (0,5 . C_D . \rho . S_M . V_M^{\,2})$$

where, C_D is the total drag coefficient, ρ is air density, S_M is the reference area of the missile and V_M is the magnitude of missile velocity. It can be seen from the Eq. 42-49 that the drag coefficient is comprised of the sum of several terms. The components of drag coefficient are: $C_{D\ body\text{-}wave}$, $C_{D\ base}$, $C_{D\ body\text{-}friction}$, $C_{D\ wing\text{-}wave}$, $C_{D\ wing\text{-}friction}$

In the simulations, drag coefficient is computed along with the instant conditions of the environment that missile flies through and the physical parameters of missile that given in Table 1.Computation of total drag coefficient is explained in Chapter III.B.1.b. in detail.

B. TARGET AIRCRAFT MODEL

In our study, high-g capacity fighter aircraft is considered as the target. Motion modeling and implementation of the target evasive maneuvers are examined by Akdağ [1]. Target equations of motion are given as:

$$V_{Tx} = V_T . \cos\gamma_T \cos\chi_T \qquad (75)$$

$$V_{Ty} = V_T . \cos\gamma_T \sin\chi_T \qquad (76)$$

$$V_{Tx} = V_T . \sin\gamma_T \qquad (77)$$

$$\dot{\gamma}_T = \frac{(L_T + u\, T_T \sin\alpha) \cos\mu}{m_T V_T} - \frac{g \cos\gamma_T}{V_T} \qquad (78)$$

$$\dot{\chi}_T = \frac{(L_T + u\, T_T \sin\alpha) \sin\mu}{m_T V_T} \qquad (79)$$

$$a_T = \frac{u\, T_T \cos\alpha - D_T}{m_T} - m_T . g . \sin\gamma_M \qquad (80)$$

where,

V_{Tx} , V_{Ty} and V_{Tz} are target velocity components,

γ_T , flight path angle χ_T , heading angle

α , angle of attack μ , and the bank angle

T_T , maximum available thrust of the aircraft L_T , the lift

m_T ,the mass of the aircraft u , throttle setting

C. SIMULATION SCENARIOS

In all of the simulation scenarios, the final period, terminal phase of the encounter is considered, where the missile is initially flying with a supersonic velocity on collision course within some kilometers from the target aircraft.

Scenario 1:

Initial engagement conditions for Scenario 1 are given as:

Missile	Target
positions on x, y, z: (0, 2000m, 2000m)	positions on x, y, z: (12000m, 0,5000m)
heading, $\chi_M = 0°$	heading, $\chi_T = 0°$
flight path angle, $\gamma_M = 0°$	flight path angle, $\gamma_T = 0°$
initial velocity = 1000 m/sec.	initial velocity = 300 m/sec.

Missile and target trajectories are evaluated with the initial conditions given above and while the target is employing Barrel Roll, Linear Acceleration, Immelmann, Horizontal-S and Split-S evasive maneuvers, respectively. Missile and target trajectories are given in Fig.18-22.

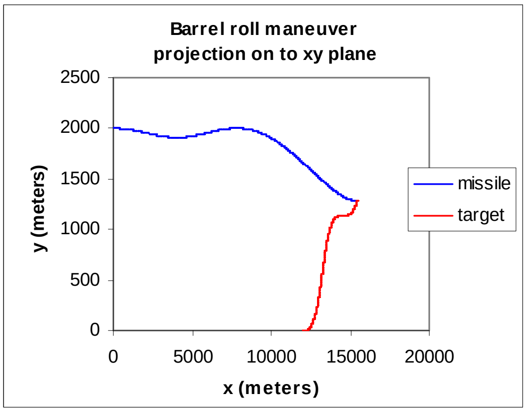

*(a) Missile-Target Trajectory Projections onto **xy**-Plane*

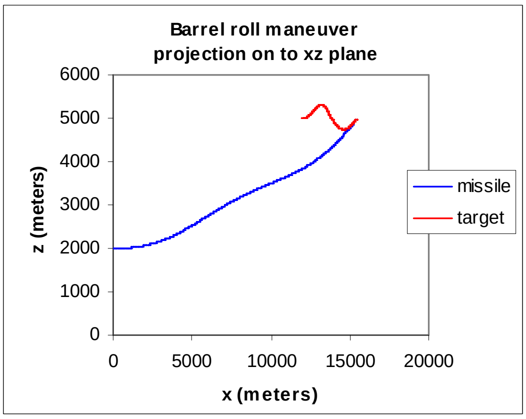

*(b) Missile-Target Trajectory Projections onto **xz**-Plane*

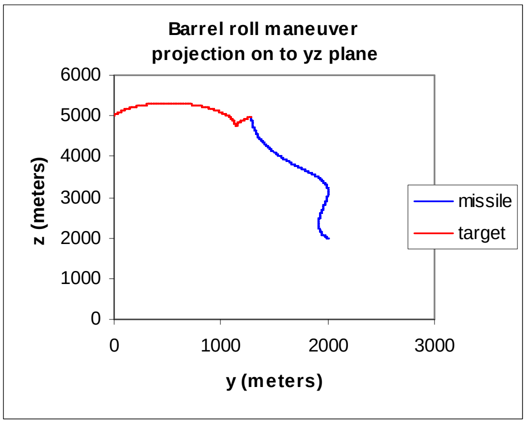

*(c) Missile-Target Trajectory Projections onto **yz**-Plane*

Figure 18 Missile-Target Trajectories of Scenario 1, Barrel Roll

When the target employs Linear Acceleration maneuver:

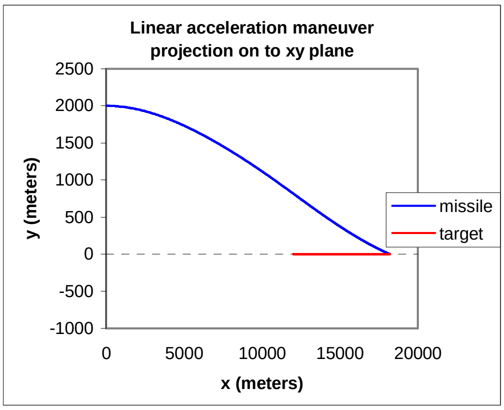

(a) Missile-Target Trajectory Projections onto ***xy****-Plane*

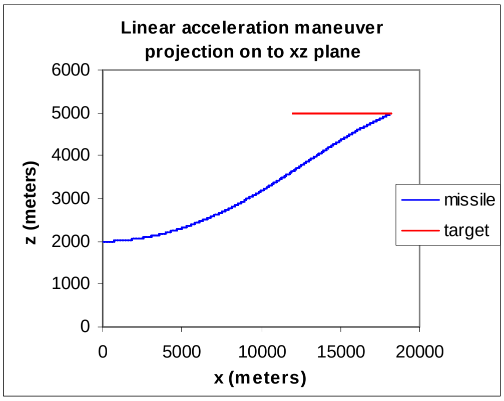

(b) Missile-Target Trajectory Projections onto ***xz****-Plane*

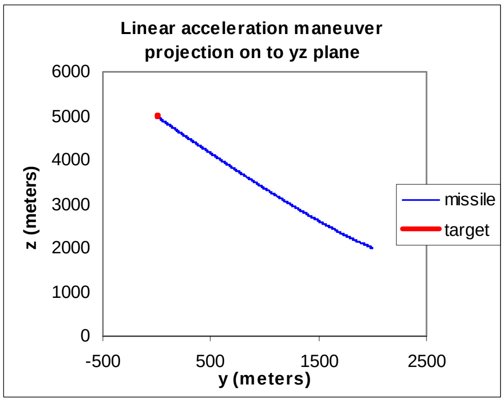

(c) Missile-Target Trajectory Projections onto ***yz****-Plane*

Figure 19 Missile-Target Trajectories of Scenario 1, Linear Acceleration

When the target employs Immelmann maneuver:

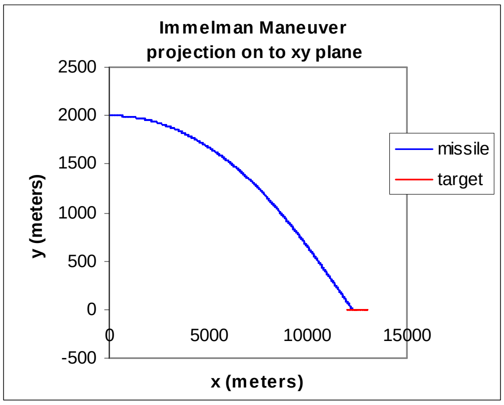

*(a) Missile-Target Trajectory Projections onto **xy**-Plane*

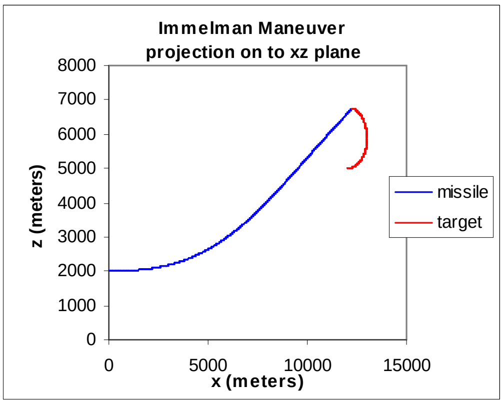

*(b) Missile-Ttarget Trajectory Projections onto **xz**-Plane*

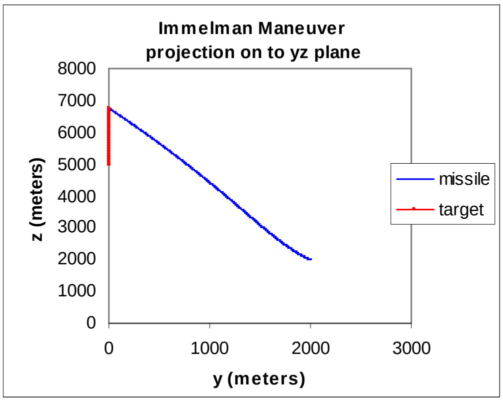

*(a) Missile-Target Trajectory Projections onto **yz**-Plane*

Figure 20 Missile-Target Trajectories of Scenario 1, Immelmann

When the target employs Horizontal-S maneuver:

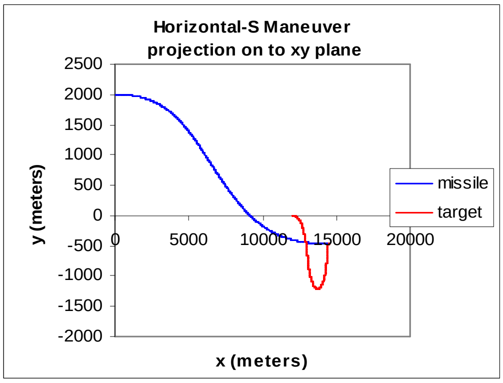

*(a) Missile-Target Trajectory Projections onto **xy**-Plane*

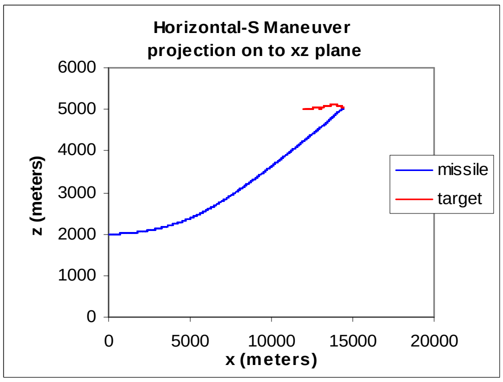

*(b) Missile-Target Trajectory Projections onto **xz**-Plane*

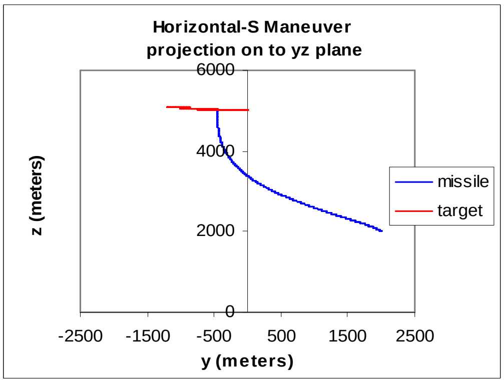

*(c) Missile-Target Trajectory Projections onto **yz**-Plane*

Figure 21 Missile-Target Trajectories of Scenario 1, Horizontal-S

When the target employs Split-S maneuver:

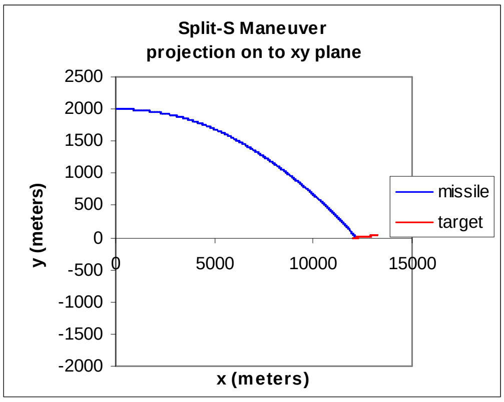

*(a) Missile-Target Trajectory Projections onto **xy**-Plane*

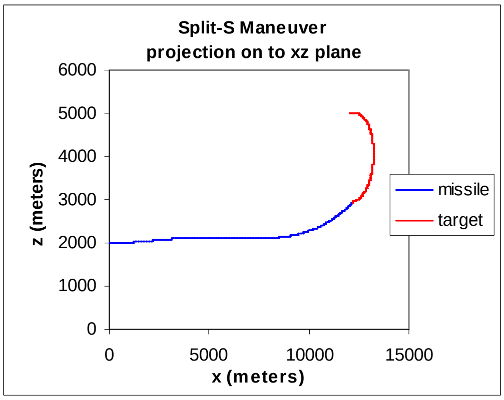

*(b) Missile-Target Trajectory Projections onto **xz**-Plane*

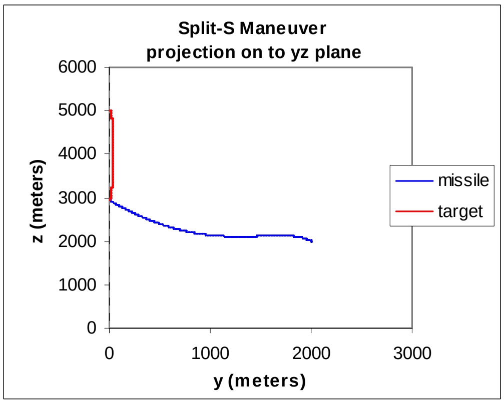

*(c) Missile-Target Trajectory Projections onto **yz**-Plane*

Figure 22 Missile-Target Trajectories of Scenario 1, Split-S

The effects of different evasive maneuvers on the missile-target trajectories are observed below for Scenario 1. It is realized that developed guidance approach works effectively against basic evasive maneuvers such as Barrel Roll, Linear Acceleration, Immelmann, Horizontal-S and Split-S.

As mentioned before, PN guidance law works by regulating the line-of-sight rate (LOSR) to zero. Missile line-of-sight angles (λ_{xy}, λ_{xz} and λ_{yz}) and deviation of line-of-sight rates ($\dot{\lambda}_{xy}$, $\dot{\lambda}_{xz}$ and $\dot{\lambda}_{yz}$) during missile flight are shown for our approach, TPA in Fig.23 and Fig.24. The target employs Horizontal-S maneuver in this engagement.

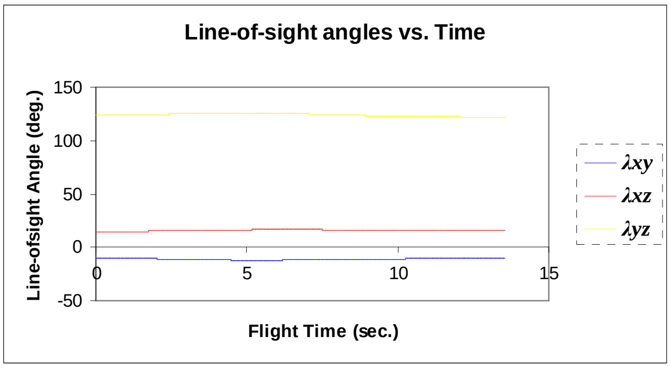

Figure 23 Line-of-sight Angles due to Flight Time

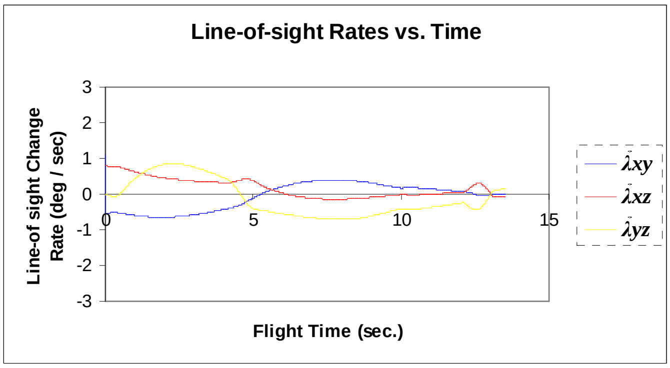

Figure 24 Line-of-sight Change Rates due to Flight Time

From Fig.23 and Fig.24, it can be seen that line-of-sight rates (LOSR) come near to zero during the missile flight. This means the target and the missile are on collision course. If to give one more example about the same subject in another scenario;

Scenario 2:

the missile initial positions are: (0, 2000m, 2000m)

the target initial positions are: (2000m, 0, 5000m)

flight path and heading angle of both the missile and the target are zero degree.

Line-of-sight angles and change rates are given in Fig.25 and Fig.26.

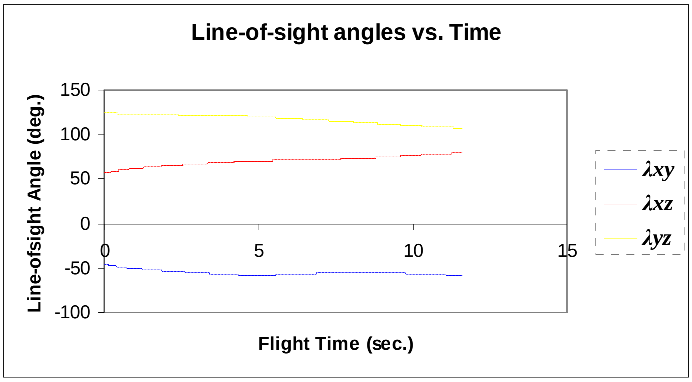

Figure 25 Line-of-sight Angles due to Flight Time (Scenario 2)

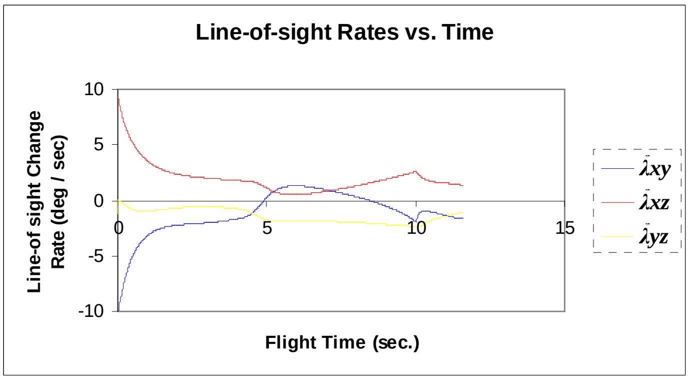

Figure 26 Line-of-sight Change Rates due to Flight Time(Scenario 2)

In the Scenario 2, since the initial range is smaller than in Scenario 1, magnitudes of line-of-sight change rates are bigger than those in Scenario 1, at the beginning of the engagement. But line-of-sight rates in Scenario 2 come to near zero, as well.

This feature of our algorithm TPA, making the line-of-sight rates in three planes come to zero, makes our pursue idea stronger.

The effects of evasive maneuvers on significant missile parameters like vertical acceleration, lateral acceleration, flight path angle (γ_M) and heading angle (χ_M) are shown in Fig.27-Fig.30

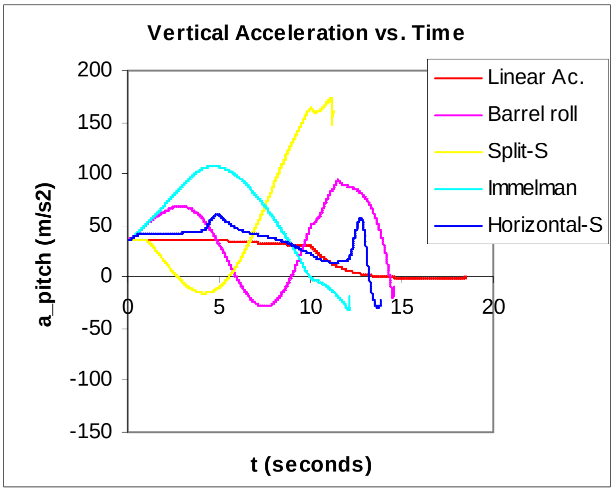

Figure 27   Missile Vertical Acceleration Magnitudes vs. Time

From Fig. 27, it can be seen that Split-S maneuver forces the missile to generate largest vertical accelerations (***a***a_{pitch}) while Linear Acceleration maneuver does smallest magnitudes. Vertical acceleration requirement against Linear Acceleration and Horizontal-S maneuver is observed low as expected. It is also seen that when the target employs Immelmann and Barrel Roll maneuver, there exist considerable vertical acceleration requirements of the missile.

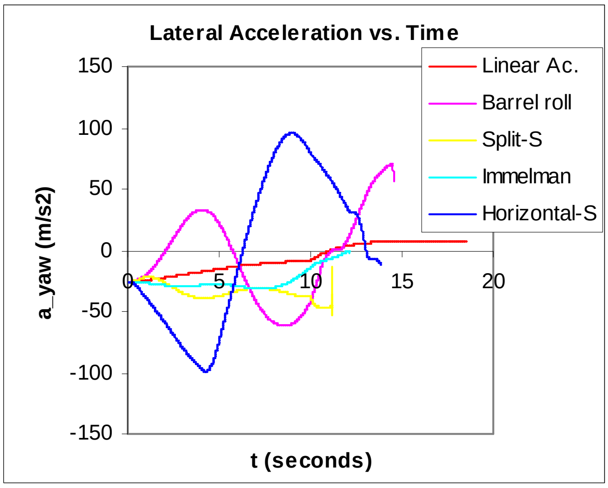

Figure 28 Missile Lateral Acceleration Magnitudes vs. Time

Lateral acceleration (***a****yaw*) magnitudes that generated against different evasive maneuvers are shown in Fig.28. It can be seen that hardest maneuver to force the missile to maximum lateral accelerations is Horizontal-S maneuver. Barrel Roll maneuver has also significant impact on it. The others have relatively negligible impact.

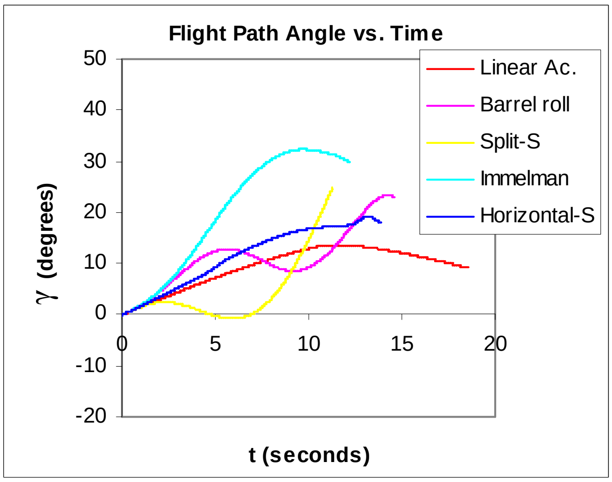

Figure 29 Missile Flight Path Angle vs. Time

A state variable, flight path angle (γ_M) magnitudes with respect to flight time are shown in Fig.29

The maneuver that forces the missile to employ maximum flight path angle is seen as Immelmann maneuver. Split-S maneuver has also strong impact on flight path angle.

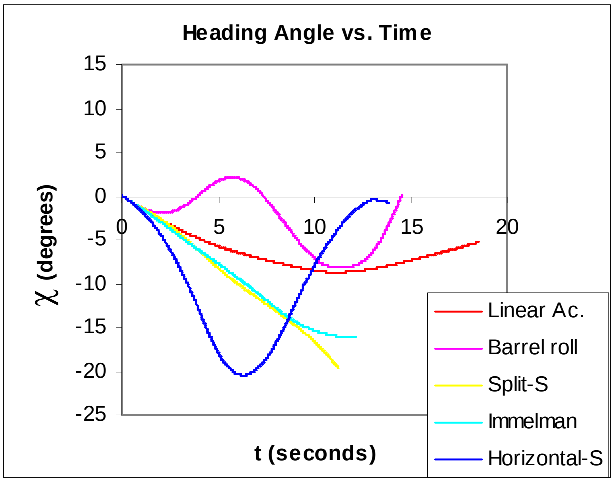

Figure 30   Missile Heading Angle vs. Time

Heading angle (χ_M) variations are shown with respect to flight time in Fig.30. Split-S and Immelmann maneuvers have linear effects on χ_M. Horizontal-S maneuver forces missile to make maximum heading. Barrel Roll and Linear Acceleration maneuvers have relatively slight effect on heading angle.

Scenario 3:

For an anti-air missile; the meaning of initial conditions such as initial position and target line-of-sight are very critical in an engagement. To evaluate the results of possible situations of both missile and the target, heading angles of both side are varied in Scenario 3. The target employs Barrel Roll maneuver. Missile's heading angle varies from −30° to +30° with the intervals of 10° while the target's heading angle varies from 0° to 180° with the intervals of 15°. Other initial conditions are given below:

Missile

positions on $\boldsymbol{x}, \boldsymbol{y}, \boldsymbol{z}$: (0, 0, 2000m)

missile heading, $= -30° < \chi_M < 30°$

flight path angle, $\gamma_M = 0°$

initial velocity = 1000 m/sec.

Target

positions on $\boldsymbol{x}, \boldsymbol{y}, \boldsymbol{z}$: (9000m, 0,2000m)

target heading, $0° < \chi_T < 180°$

flight path angle, $\gamma_T = 0°$

initial velocity = 300 m/sec.

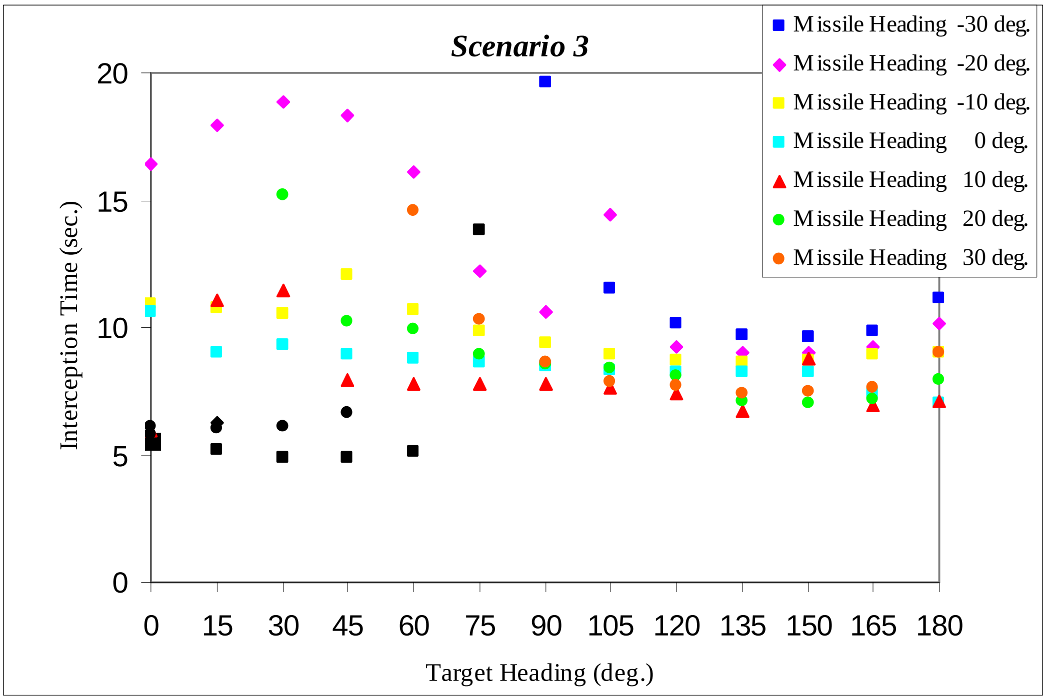

Figure 31 Interception Time due to Missile and Target Heading Angles

From Fig.31 it can be easily seen that interception time increases with relative heading angle magnitude. For example, when the missile heading is equal to zero, means the target is in front of the missile, interception time is very small whatever the target heading is. But when the missile heading is equal to −30° or −20° the interception time increases or the mission results with miss. Black points in Fig.31 represent the misses.

Scenario 4:

In this scenario, the performance of developed approach, TPA, is compared with the PN method widely used in the literature [23, 38, 39, 40]. As mentioned in Chapter IV, in this method, vertical and lateral acceleration components are computed differently (Eq.64-Eq.65) from those computed in TPA.

The scenario is given as:

<u>Missile</u>

positions on ***y***, ***z***: (2000m, 2000m)

heading, $\chi_M = 0°$

flight path angle, $\gamma_M = 0°$

initial velocity = 1000 m/sec.

<u>Target</u>

positions on ***x***, ***y***, ***z***: (14000m, 0,2000m)

heading, $\chi_T = 0°$

flight path angle, $\gamma_T = 0°$

initial velocity = 300 m/sec.

To compare the results of both methods, TPA and PN; the ***x*** position of missile is varied from origin to 10000 meters with the intervals of 250 meters. The simulation is run for TPA and PN for the target employing basic evasive maneuvers. The results are given in Fig.32-Fig.36.

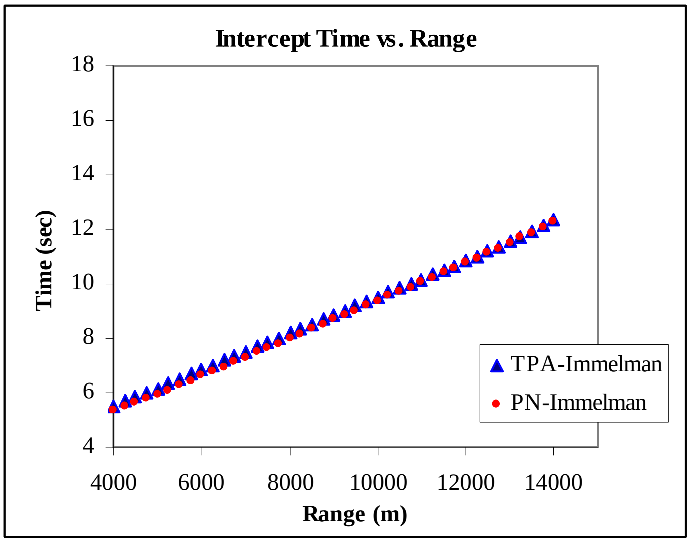

Figure 32 Evaluation of TPA with PN, Immelmann Maneuver

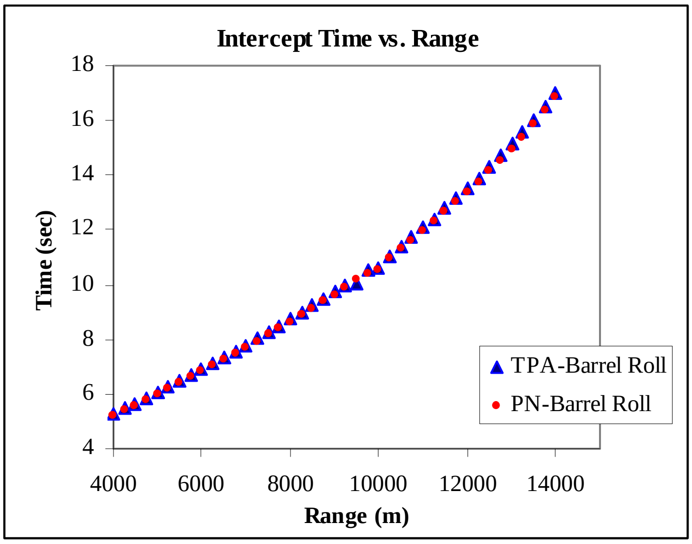

Figure 33 Evaluation of TPA with PN, Barrel Roll Maneuver

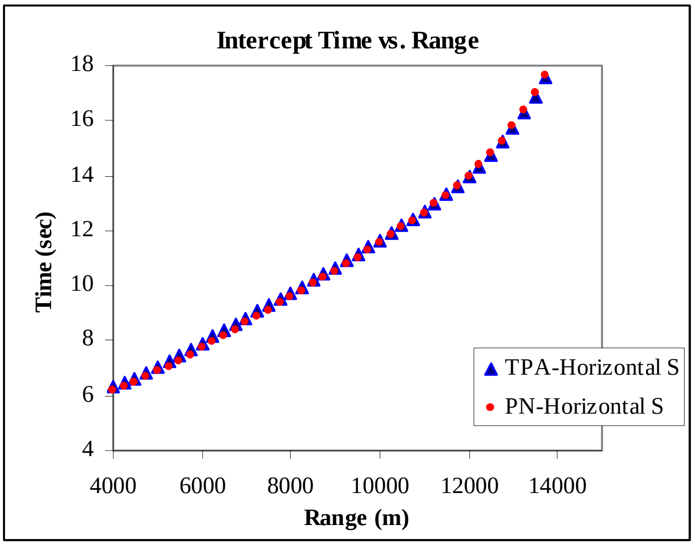

Figure 34 Evaluation of TPA with PN, Horizontal S Maneuver

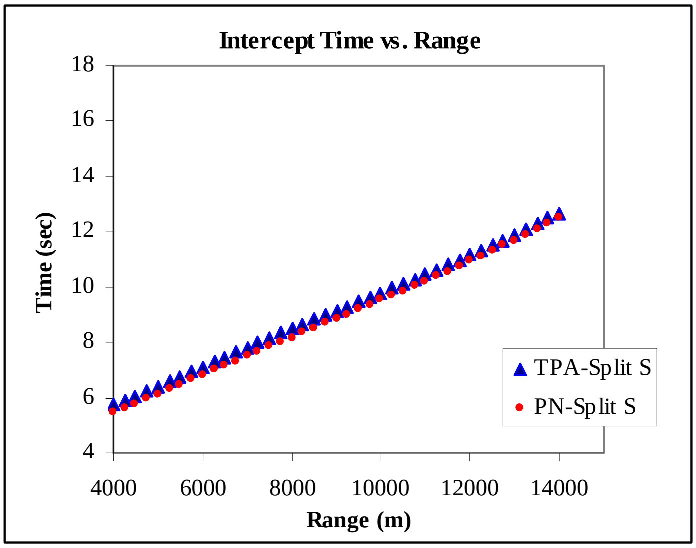

Figure 35   Evaluation of TPA with PN, Split S Maneuver

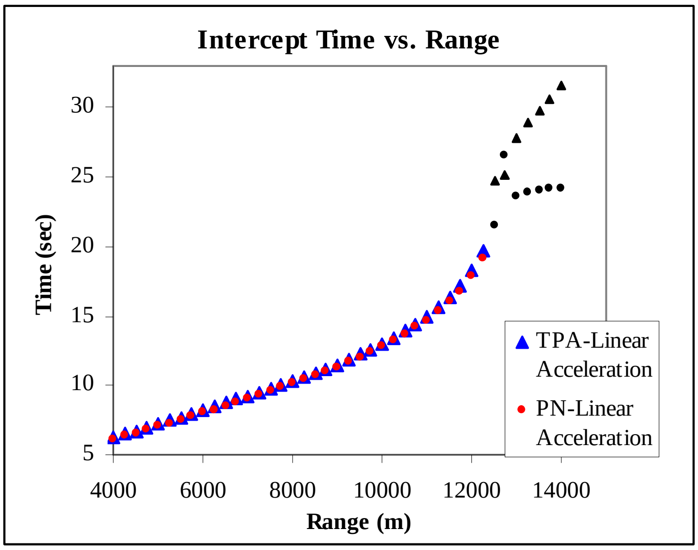

Figure 36   Evaluation of TPA with PN, Linear Acceleration Maneuver

Black points in Fig.36 represent the miss conditions. It could be seen from the simulation results that; the interception time due to range magnitudes for PN and TPA methods are very close to each other. (Fig.32-Fig.36)

VII. CONCLUSION AND FURTHER RESEARCH

As the main contribution this thesis; a novel guidance approach for 3D missile guidance is developed, which is effective against high-g capability fighter aircrafts that employ evasive maneuvers. The performance of this approach has been tested both visually and analytically via developed simulation software, VEGAS (Visual End-Game Simulation). When compared with classical PN approach, it is verified that the performance of proposed approach is robust and effective for high-g capacity aerial targets employing evasive maneuvers.

VEGAS is constructed as a production of this thesis. Different modules of this simulator have been designed, developed and implemented by Moran and Akdağ [1] as parts and partials of their master thesis projects. From the viewpoint of the missile, a large number of missile parameters are included into “pursuer” module of VEGAS. Thus, it is possible to evaluate the performance of any missile configurations by changing only the parameters of the “pursuer” module of VEGAS. Since it is designed in a modular and visual structure, it may also be used as a training tool by the related army staff.

In this study, the missile is assumed to have perfect knowledge of target position. In a real situation, there are likely to be measurement errors in the missile’s measurement of the target aircraft data such as position, closing velocity etc. Although “radar” module produces perfect map of engagement space upon the requests from missile, the module structure is designed to support producing signal superimposed with noise.

Only the missile motion dynamics of the encounter are considered in this study. However, in a real encounter, the target aircraft is probable to have countermeasures, such as chaff. In such a situation, missile guidance system is expected to filter the fake data by using extended techniques like Kalman Filtering and to guide the missile to the real target position to intercept.

Additionally, in a possible missing occurrence, the missile should have re-attack capability by using an extra algorithm if its propellant quantity is sufficient for a new attack.

Trajectory learning and optimization using neural networks will also be included into the guidance system. Missile guidance system will be trained via specific target maneuver data. Hence the missile and its guidance system will be ready to make the best maneuver decision for pre-defined target maneuvers.

The modeling of the electronic counter-countermeasures, the re-attack function, trajectory learning and optimizing the use of such procedures are our directions of further research.

REFERENCES

[1] Akdağ, R., "*Evaluation of Basic Fighter Maneuvers Against Proportional Navigation Missiles*", Master Thesis, Naval Science and Engineering Institute, İstanbul, 2005 (submitted for thesis defense)

[2] Zarchan, P., "*Tactical and Strategic Missile Guidance*", 4th Ed. Tactical Missile Series AIAA Inc., Washington, D.C.,2004

[3] Locke, A.S., "*Guidance*", Van Nostrand Co., Princeton, NJ, 1955

[4] Lin, C. F., "*Modern Navigation, Guidance and Control Processing*", Volume II. Prentice Hall, 1991

[5] Cloutier, J. R., Evers, J. H., and Feeley, J. J., "*Assessment of Air-to Air Missile Guidance and Control Technology*", IEEE Control Systems Magazine, 9(6) pp. 27-34, October 1989.

[6] Lin, C. L., and Su, H. W., "*Intelligent Control Theory in Guidance and Control System Design: and Overview*", Proceedings of National Science Council ROC(A), 24 (1): pp. 15-30, 2000

[7] Shukla, U. S., and Mahapatra, P. R., "*True Proportional Navigation Dilemma – Pure or True?*" , IEEE Transactions on Aerospace and Electronic Systems,Vol.26, No.2, pp.382-392, 1990

[8] Murtaugh, S.A., and Criel, H.E., "*Fundamentals of Proportional Navigation*", IEEE Spectrum, Vol. 3, pp. 75-85. , 1966

[9] Spaceline homesite (www.spaceline.org), Spaceline Inc., Cape Canaveral, Florida.

[10] Tucker, T.W., "*Electronic Countermeasure Effectiveness Evaluation*", AOC Professional Development Course Document, Alexandria, 2000

[11] Ranta, J., "*Optimal Control and Flight Trajectory Optimization Applied to Evasion Analysis*", Licentiate Thesis, Department of Engineering Physics and Mathematics, Helsinki University of Technology, 2004

[12] Raju, P.A., Ghose, D., "*Empirical Virtual Sliding Target Guidance Law Design: An Aerodynamic Approach*", IEEE Transactions on Aerospace and Electronic Systems Vol.39, No.4, 2003

[13] Bryson, A. E., and Ho, Y. C., "*Applied Optimal Control*", Blaisdell, Waltham, MA, USA, 1969

[14] Nazaroff, G. J, "*An Optimal Terminal Guidance Law*", IEEE Trans. Automat. Contr., 21(6), pp. 407-408, 1976

[15] Potter, J. E. "A *Guidance-Navigation Separation Theorem*", AIAA Paper 64-653, AIAA, Washington DC, USA, 1964

[16] Speyer, J. L., Greenwell, W. M., and Hull, D.G., "*Adaptive Noise Estimation and Guidance for Homing Missile*", AIAA Guidance and Control Conference, Washington DC, USA, 1982

[17] Tsao, L. P., and Lin, C. S., "*A New Optimal Guidance Law for Short- Range Homing Missiles*", Proceedings of the National Science Council, Republic of China, 24(6): pp. 422-426, 2000

[18] Naeem, W., Sutton, R., Ahmad, S. M., Burns R. S., "*A Review of Guidance Laws Applicable to Unmanned Underwater Vehicles"*, Marine and Industrial Dynamic Analysis Group, The University of Plymouth, " Journal of Navigation, vol. 56, no. 1, pp. 15-29, January 2003

[19] Guelman, M., "*The Closed-Form Solution of True Proportional Navigation*", IEEE Transactions on Aerospace and Electronic Systems, Vol.12, No.4, pp.472-482, 1976

[20] Shukla, U. S., and Mahapatra, P. R., "*Generalized Linear Solution of Proportional Navigation*", IEEE Transactions on Aerospace and Electronic Systems,Vol.24, No.3, pp.231-238, 1988

[21] Mahapatra, P.R. and Shukla, U.S., "*Accurate Solution of Proportional Navigation for Maneuvering Targets*", IEEE Transactions on Aerospace and Electronic Systems,Vol.25, No.1, pp.81-89, 1989

[22] Becker, K., "*Closed-Form Solution of Pure Proportional Navigation*", IEEE Transactions on Aerospace and Electronic Systems, Vol.26, No.3, pp.526-533, 1990

[23] Yuan, P.J. and Chern, J.S., "*Solutions of True Proportional Navigation for Maneuvering and Non-maneuvering Targets*", Journal of Guidance, Control and Dynamics, Vol.15, No.1, pp. 268-271 1992

[24] Yuan, P.J. and Hsu, S. C., "*Exact Closed–Form Solution of Generalized Proportional Navigation"*, Journal of Guidance, Control and Dynamics, Vol.16, No.5, pp. 963-966, 1993

[25] Rajasekhar, V. and Sreenatha, A. G., "*Fuzzy Logic Implementation of Proportional Navigation Guidance*", Acta Astronautica, Elsevier Science Ltd., 46(1): pp. 17-24, 2000

[26] Creaser, P. A., Stacey, B. A. and White B. A., "*Evolutionary Generation of Fuzzy Guidance Laws*", UKACC International Conference on Control' 98, UK, vol. II, no. 455: pp. 883-888, 1998

[27] Menon, P. K. and Iragavarapu, V. R., "*Blended Homing Guidance Law Using Fuzzy Logic*", AIAA Guidance, Navigation and Control Conference, Boston MA, 1998

[28] Yang, C. D. and Chen, H. Y., "*Three-Dimensional nonlinear H-Infinity Guidance Law*", International Journal of Robust and Nonlinear Control, 11(2): pp. 109-129, 2001

[29] Yuan, C. L., "*Homing and Navigation Courses of Automatic Target-Seeking Devices*", RCA Labs., Rept. PTR-12C, Princeton, NJ, 1942

[30] Fossier, M. W., "*The Development of Radar Homing Missiles*", AIAA Journal of Guidance, Control and Dynamics, Vol. 7, pp 641-651, 1984

[31] Yuan, C. L., "*Homing and Navigation Courses of Automatic Target-Seeking Devices*", Journal of Applied Physics, Vol. 19, pp. 1122-1128, 1948

[32] Yuan, P.,J., "*Optimal Guidance of Proportional Navigation*", IEEE Transactions on Aerospace and Electronic Systems, Vol. 33, No.3, pp. 1007-1012, 1997

[33] Yang, C. D., Yeh, F. B. and Chen, J. H., "*The Closed Form Solution of Generalized Proportional Navigation*", IEEE Transactions on Aerospace and Electronic Systems, Vol. 10, No.2, pp. 216-218, 1987

[34] Chakravarthy, A., Ghose, D., "*Capturability of Realistic Generalized True Proportional Navigation*", IEEE Transactions on Aerospace and Electronic Systems, Vol.32, No.1, pp.407-418, 1996

[35] "*ISO Standard Atmosphere*", International Organization for Standardization, ISO 2533:1975

[36] Derr, V.E., "*Atmospheric Handbook: Atmospheric Data Tables Available on Computer Tape"*, World Data Center A for Solar-Terrestrial Physics, Report UAG-89, Boulder, Colorado, 1984

[37] Fleeman, E. L., "*Tactical Missile Design*", Education Series, AIAA Inc., Reston, Virginia, 2001

[38] Choi, H.L., Bang, H.C., Tahk, M.J., "*Co-evolutionary Optimization of Three-Dimensional Target Evasive Maneuver Against a Proportionally Guided Missile*", IEEE, Proceedings of the 2001 Congress on Evolutionary Computation, pp. 1406-1413, 2001

[39] Raivio, T., Ranta, J., "*Optimal Missile Avoidance Trajectory Synthesis In The Endgame*", AIAA Guidance, Navigation, and Control Conference and Exhibit, California, 2002

[40] Hytönen, H., "*Utilization of Air-To-Air Missile Seeker Constraints In The Missile Evasion*", Independent Research Project in Applied Mathematics, 2004

[41] Miele, A., "*Flight Mechanics*", Addision Wesley, Massachusetts, MA, 1962.

APPENDIX-1: PUBLICATIONS

Moran, İ., Altılar, D. T., "*Three Plane Approach for True Proportional Navigation*", American Institute of Aeronautics and Astronautics; Guidance, Navigation, and Control Conference and Exhibit, California, 15-18 August 2005.